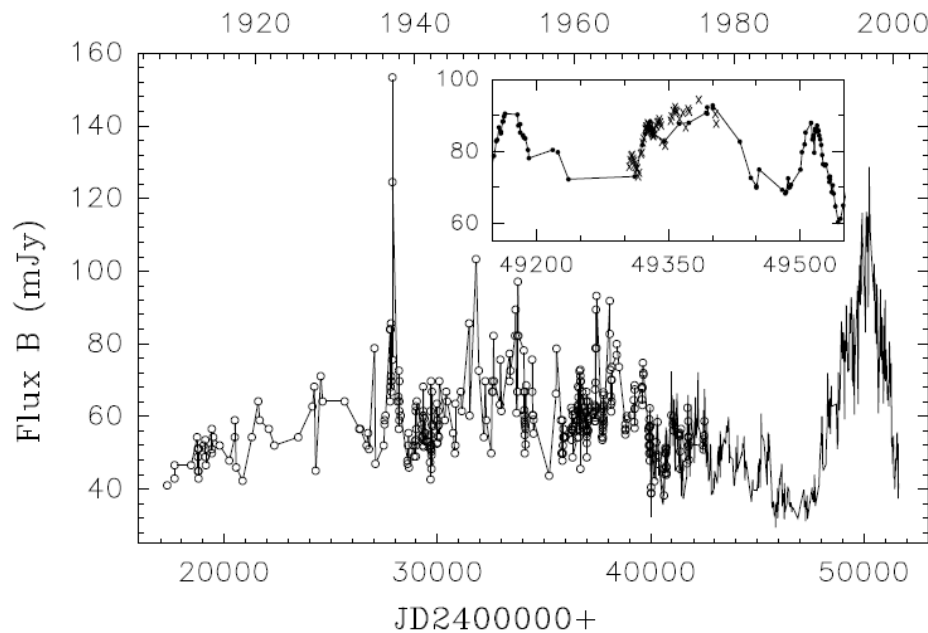


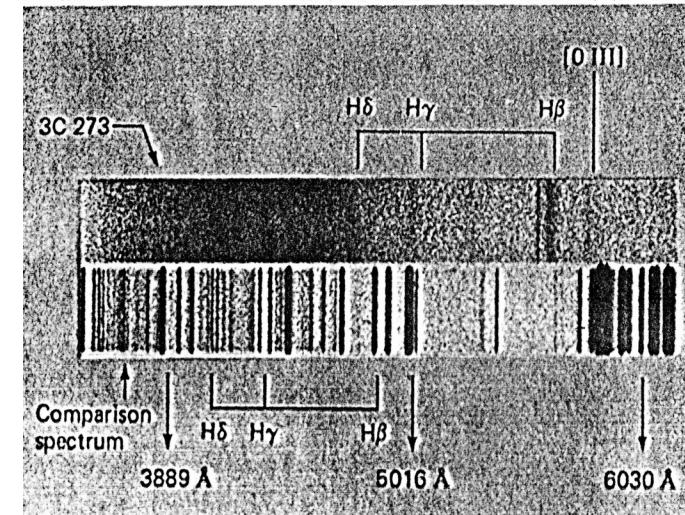
# Applications: active galactic nuclei

## 1. Historical comment about AGN

We talked briefly about the history of the discovery of quasars during Lecture 1. That happened in 60" of the past century. But studies of AGN have much longer history.



**Figure 1.** The light curve of NGC 4151 in the *B* band from the historical plate data (open circles connected with a continuous line) and Crimean observations (solid line). The inserted expanded fragment shows the AGN Watch data (crosses) together with the Crimean data (continuous line). The



*The optical spectrum of 3C 273 from Schmidt (1963)*

This is for example the lightcurve of NGC 4151 which I used for the variability study. It starts at 1910.

The source was first mentioned by William Herschel on March 17, 1787, later classified in the old times as a nebula, and contained in one of subsequent versions of the **New General Catalogue** (NGC) published in 1888-1908 by John Dreyer.

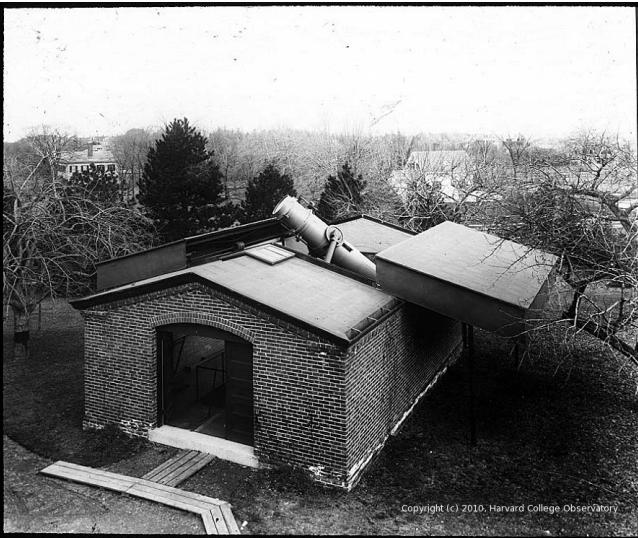
# 1. Historical comment about AGN

To learn what your favorite object did during the last 100 years you can now go to the project page:

## DASCH: Digital Access to a Sky Century @ Harvard A New Look at the Temporal Universe

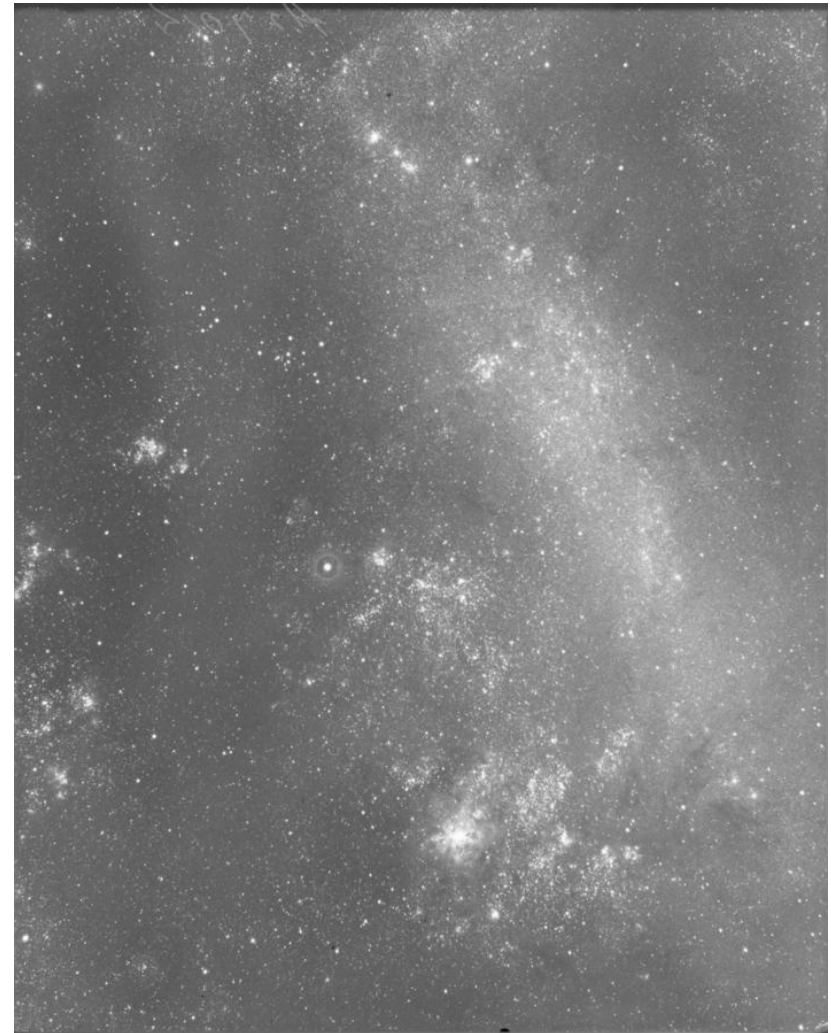
<http://dasch.rc.fas.harvard.edu/project.php>

The collection of glass plates contains over 500,000 images, covering both the northern and southern hemispheres, and spanning the years 1882-1992.



The plates were taken with different telescopes, with the first one being the **24 inch Bruce Doublet** telescope, operating first in Cambridge (1893 to 1895), then moved to Peru.

*Plate a27014 of Large Magellanic Cloud taken on October 27, 1949 from Bloemfontein, South Africa, with the 24 inch Bruce Doublet. The exposure was 60 minutes centered on 5h25m23s R.A. and -68d55m01s Declination.*



# 1. Historical comment about AGN

## DASCH: Digital Access to a Sky Century @ Harvard A New Look at the Temporal Universe

Software allows to create lightcurves for selected objects. Here is an example of the long term behaviour of three binary systems in M44 (Tang, Grindlay et al. 2010).

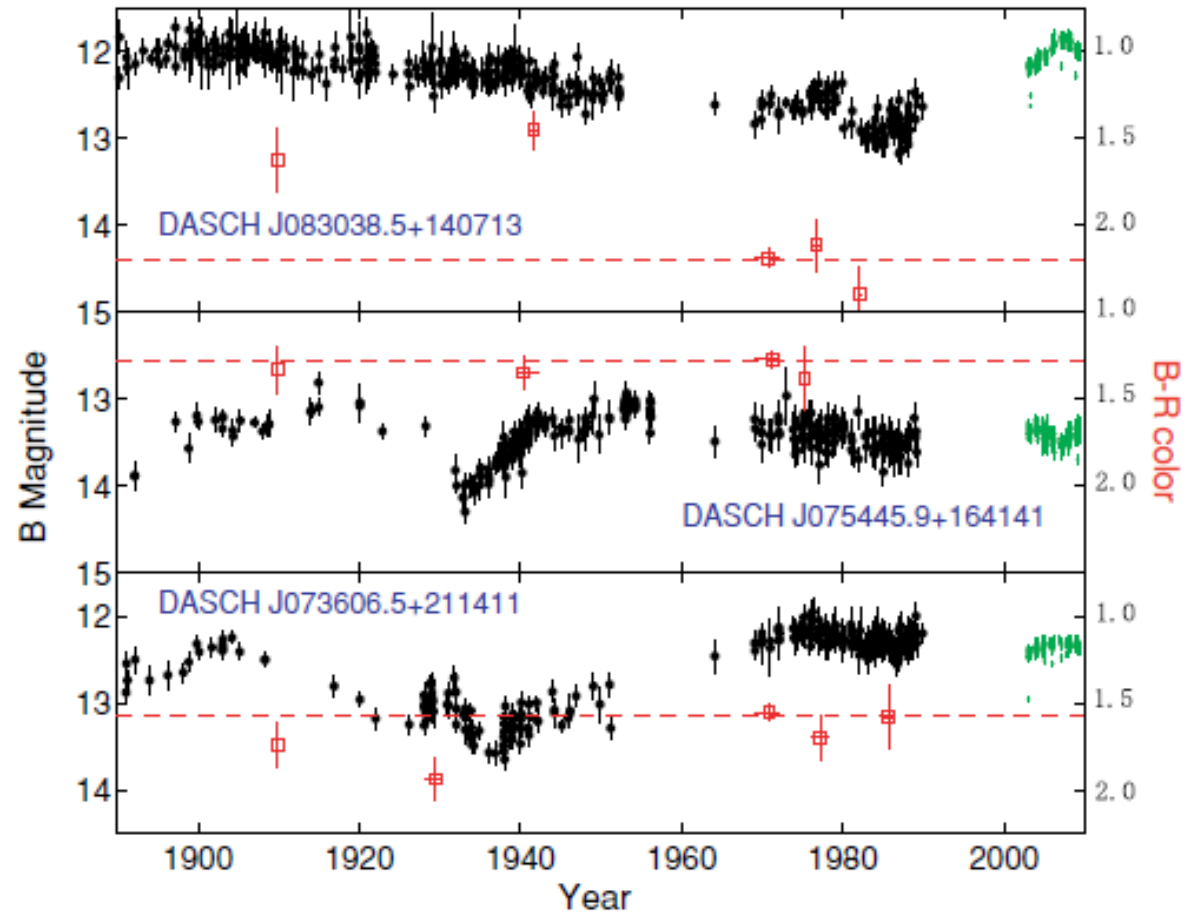


**Figure 1.** Light curves and color evolution of three unusual long-term variables which were found in DASCH scans near M44. Black dots with error bars are the light curves from DASCH, small green dots are the light curves from ASAS. Since ASAS data are in  $V$  band, while DASCH magnitudes are  $B$ , we added 1.16 mag to the ASAS  $V$  mag in the plots which is the mean  $B - V$  value for K2III stars (Cox 2000). Red open squares are the  $B - R$  color derived from plates with the y-axis labeled in the right, and red dashed lines mark the weighted mean  $B - R$  color values from 1970s to 1980s.



# 1. Historical comment about AGN

Other early discovery: around 1920, discovery of BL Lac (BL variable star in the constellation of Lacerta), still without proper recognition of the issue.

First essential step:

Carl Seyfert, 1943, “ Nuclear emission in spiral nebulae” (NGC 4151, NGC 1068, NGC 7469, NGC 3516 i NGC 1275) – his attention was called by the exceptionally bright nuclei of these galaxies, and their vary broad and intense emission lines.

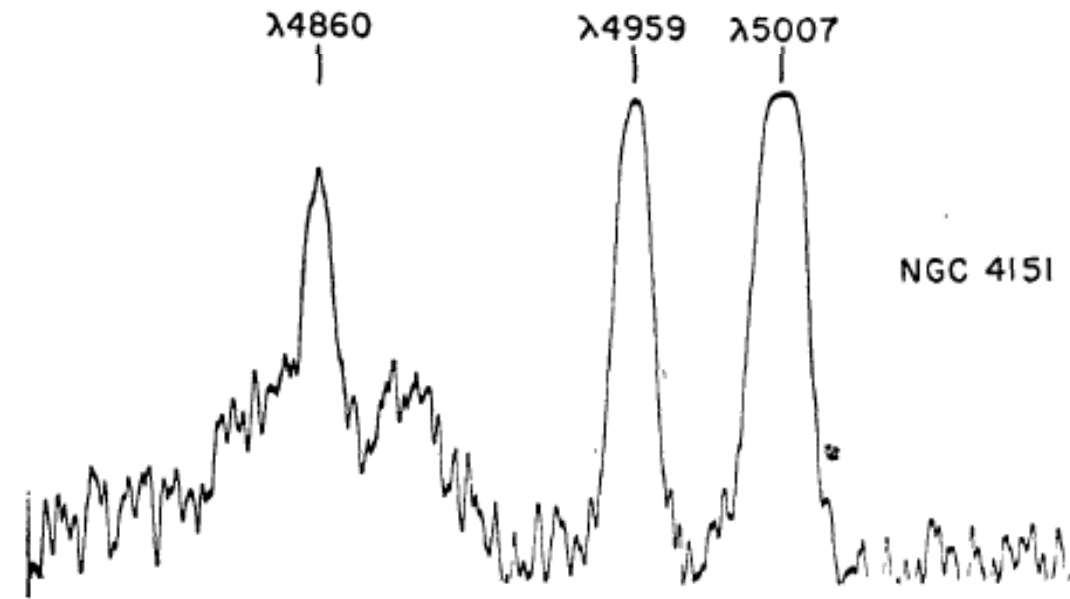


FIG. 1.—Microphotometer tracings of the emission lines  $\lambda\lambda$  4860 ( $H\beta$ ), 4959 and 5007 [ $O\ III$ ] in the nebulae NGC 1068, 3516, and 4151.

*From original paper of Seyfert (1943).*

# 1. Historical comment about AGN

Carl Seyfert, 1943, “ Nuclear emission in spiral nebulae“ (NGC 4151, NGC 1068, NGC 7469, NGC 3516 i NGC 1275) – his attention was called by the exceptionally bright nuclei of these galaxies, and their vary broad and intense emission lines.

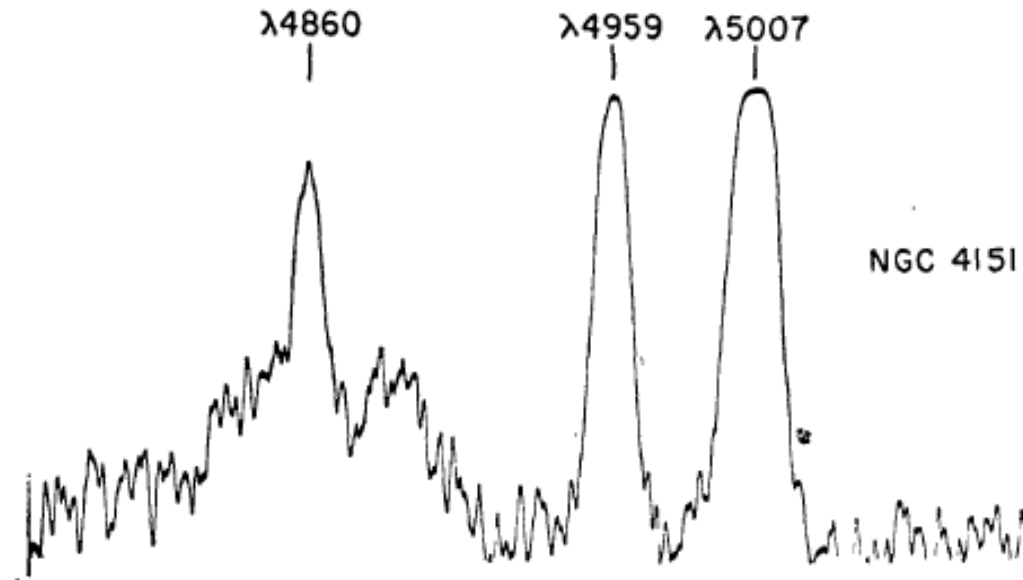
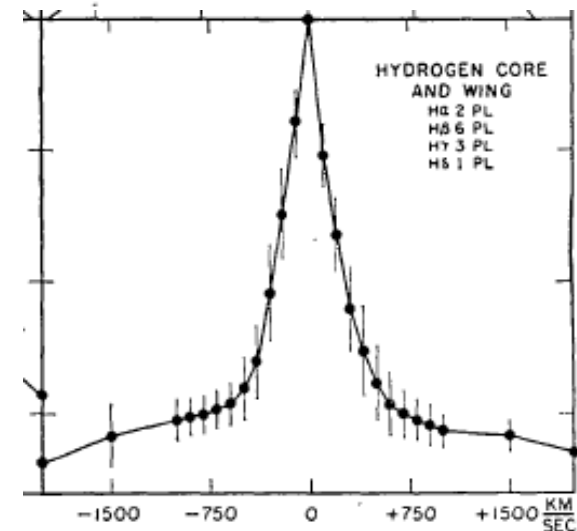


FIG. 1.—Microphotometer tracings of the emission lines  $\lambda\lambda$  4860 ( $H\beta$ ), 4959 and 5007 [O III] in the nebulae NGC 1068, 3516, and 4151.

He was brave enough to claim the real width of the Hbeta line in NGC 4151; in the abstract he gives 7500 km/s as the zero level width of the wings; we know now that FWHM of the broad component of the line is for example 3200 km/s as measured in 2002 by Shapovalova.

*From original paper of Seyfert (1943).*



## 2. Digression: emission lines

### 2.1 Hydrogen atom

Hydrogen is the most abundant element, and if the conditions are appropriate (temperature of order of a few thousands of degrees) it is a source of strong lines.

Hydrogen atom consists of a single proton (nucleus), and a single electron, and it is easy to calculate the possible energy states of such an atom within the frame of quantum theory. We have to solve the time-independent Schroedinger equation

$$H \psi = E \psi$$

Here  $\psi$  is the wave function of the electron, H is an operator

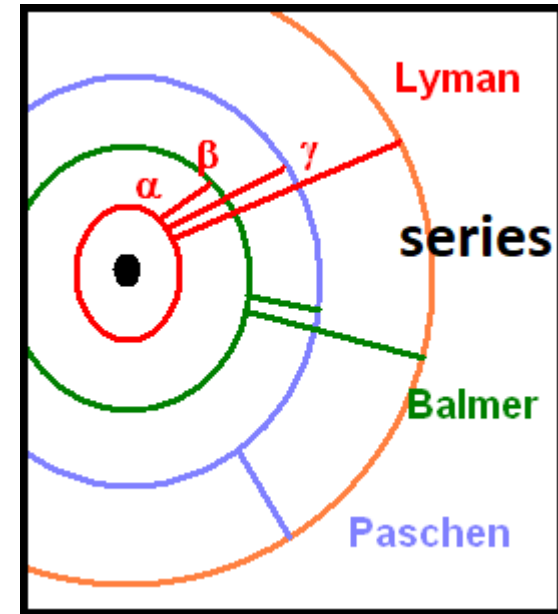
$$H = -\frac{\hbar^2}{2m} \nabla^2 - \frac{e^2}{r};$$

We neglect here relativistic effects as well as spin effects. We can solve this equation assuming separation of r and angular dependences

$$\psi = \frac{1}{r} R(r) Y(\theta, \phi);$$

The solution gives finally the energy levels of the atom:

$$E_n = \frac{e^2}{2 a_0 n^2} = -13.6 eV \frac{1}{n^2}$$



Energy levels are given either in energy units, or the corresponding wavelength:

$$\lambda = c / \nu; E = h \nu; 1 \text{ \AA} = 10^{-8} \text{ cm}$$

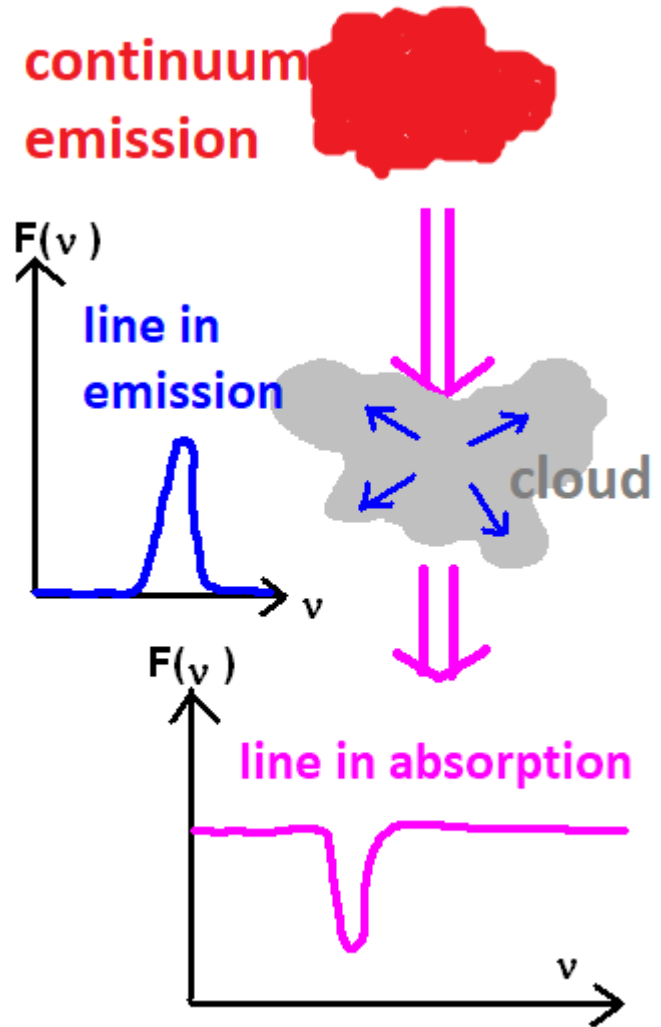
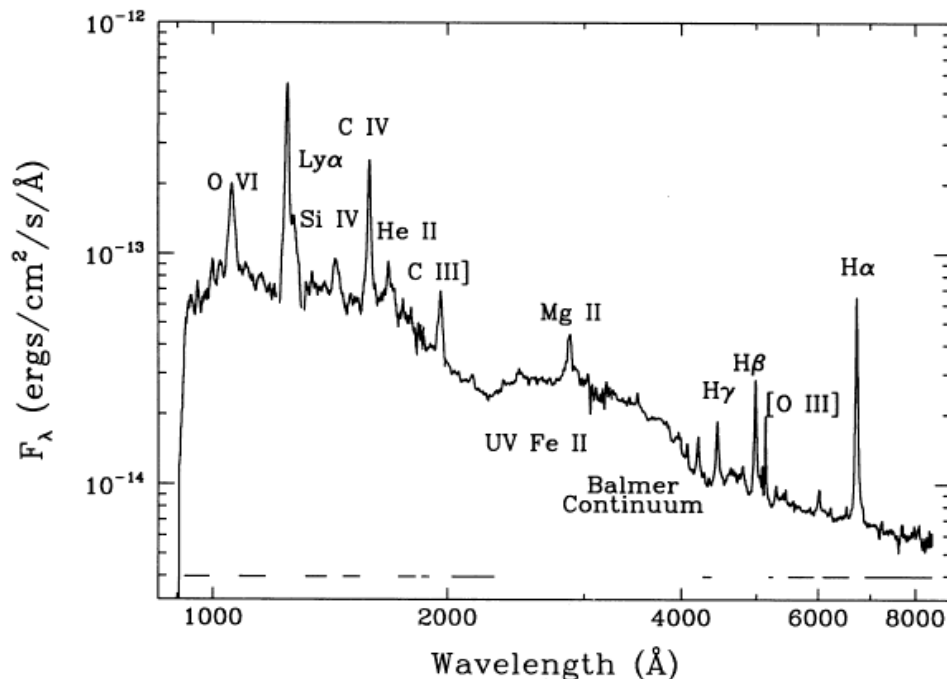
Ly $\alpha$	- 1216 \AA	Lyman	UV
H $\alpha$	- 5563 \AA	Balmer	opt
H $\beta$	- 4861 \AA	"	opt
H $\gamma$	- 4340 \AA	"	opt
Pa $\alpha$	-	Paschen	IR

## 2. Digression: emission lines

### 2.2 Formation of emission and absorption lines

If we have a source of continuum emission, and a hydrogen cloud located at some distance, the results depend on the location of an observer.

Photons with energies roughly corresponding to the excitation levels are efficiently absorbed, electrons go to excited levels, and in most cases deexcitation happens through emission of photons, but this time photons are reemitted isotropically (sometimes deexcitation happens through collisions).

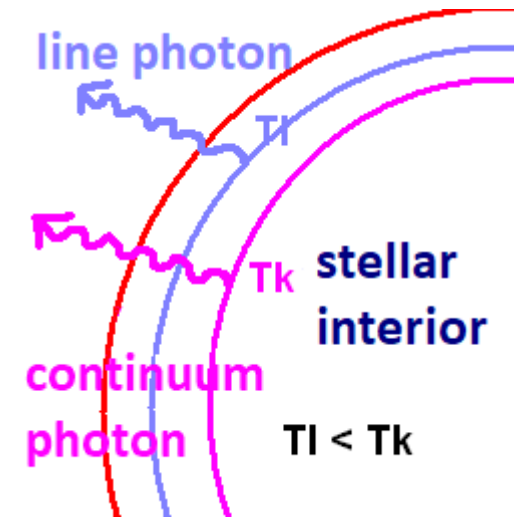


In AGN we mostly see emission lines. This immediately implies that the emitting material is not located along our line of sight to the continuum.

*The spectrum of Mrk 335, Zheng et al. 1995*

## 2. Digression: emission lines

In real situations due to more subtle effects both emission and absorption lines can be seen in the spectrum. For example, Sun spectrum contains mostly absorption lines which form due to the drop of the temperature outward and a corresponding decrease of the emissivity with height. But also faint emission lines form, and this happens in the solar chromosphere, when the temperature rises outwards and the atmosphere meets the solar corona. There, the enhanced dissipation leads to formation of emission lines.



### 2.3 Emission line widths

Line widths are determined by the physics and the motion of the medium:

(a) natural line width -  $\Delta E \times \Delta t > h$

Typically the lifetime of the level is  $10^{-8}$  s, the corresponding energy uncertainty about  $10^{-9}$  eV, and the corresponding velocity is about **1 m/s**. Negligible.

(b) collisional broadening  $\frac{\Delta \lambda}{\lambda} = \frac{v}{c} = \sqrt{\frac{kT}{mc^2}}$

(c) thermal broadening -

The temperature cannot be higher than 5 000 K (0.5 eV), and the thermal velocity corresponding to it is about 300 km/s. **Small**.

(d) kinematic broadening (turbulent, or due to the systematic motion)

**Line widths of order of thousands km/s as in AGN must be due to kinematic motion.**



## 2. Digression: emission lines

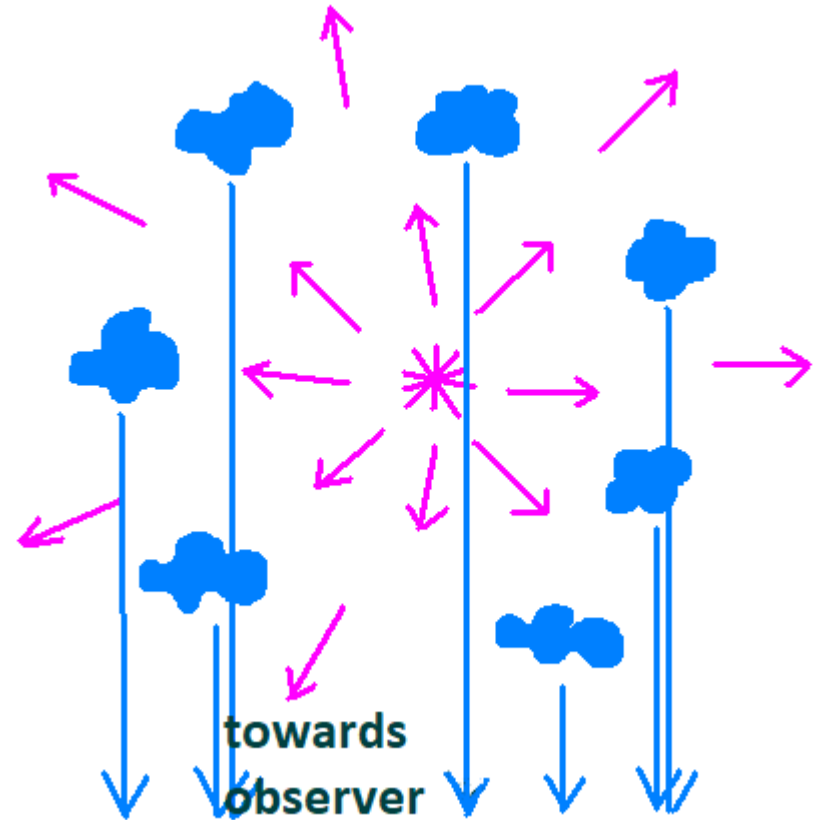
### 2.4 Emission line intensity

Line intensity also contains important information about the physics and geometry of the emitting medium.

For example, if we have a source of continuum (magenta) which irradiates a number of clouds which are not along the line of sight to the observer then the expected emission line, for example H $\beta$ , is given by the thermal conditions in the irradiated clouds,  $A$ , the source total continuum luminosity,  $L$ , and the covering factor of the source sky by the clouds,  $f$ .

Most difficult is computing the response of a single cloud to irradiation since this requires computing the thermal and ionization balance in the cloud, this in turn requires assumption of the cloud structure (constant density ? constant pressure ?) and solving the radiation transfer through the cloud.

$$L_{H\beta} = A(\text{physics}) L_{tot} f; \quad A(\text{physics}) - \text{probability of } H\beta \text{ emission}$$



**Complex codes are used for that purpose, the most popular one is the code CLOUDY by Gary Ferland and collaborators.**

### 3. AGN basic classification

This is a very complex issue, some aspects seem to be well understood, some are still under discussion.

**AGN**

**Radio-loud (jetted) objects**

**Radio-quiet objects**

**RL quasars  
(brigher)**

**radio-  
galaxies  
(fainter)**

**RQ quasars  
(brigher)**

**Seyfert  
galaxies  
(fainter)**

This sub-division into quasars and galaxies are mostly historical (optically resolved versus unresolved host galaxy) and unnecessary from the point of view of the AGN understanding but it is still frequently used.

The division into jetted and not-jetted sources is important.

## 4. Jetted sources

In the case of sources with strong jets, the view dramatically depends on the source orientation. When jet emit directly towards us like in 3C 279, the most famous blazar, the broad band spectrum is dominated by jet emission:

synchrotron and Compton component

During the outburst the accretion disk and the Broad Line Region component is not seen, but when caught in the **faint state**, the quasar shows steep spectrum but with very nice BLR.

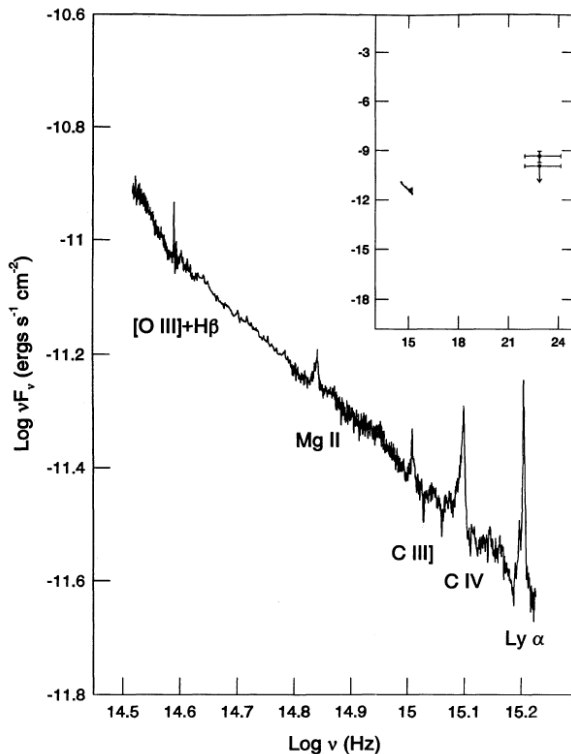


FIG. 1.—The 1992 April multiwavelength spectrum of 3C 279. The insert shows the combined optical-ultraviolet- $\gamma$ -ray spectrum with the EGRET points from Kniffen et al. (1993), with the flux density uncertainty and the EGRET energy band indicated. A reddening correction corresponding to  $E(B-V) = 0.015$  has been applied to the optical-ultraviolet data (Burstein & Heiles 1992).

Netzer et al. 1994

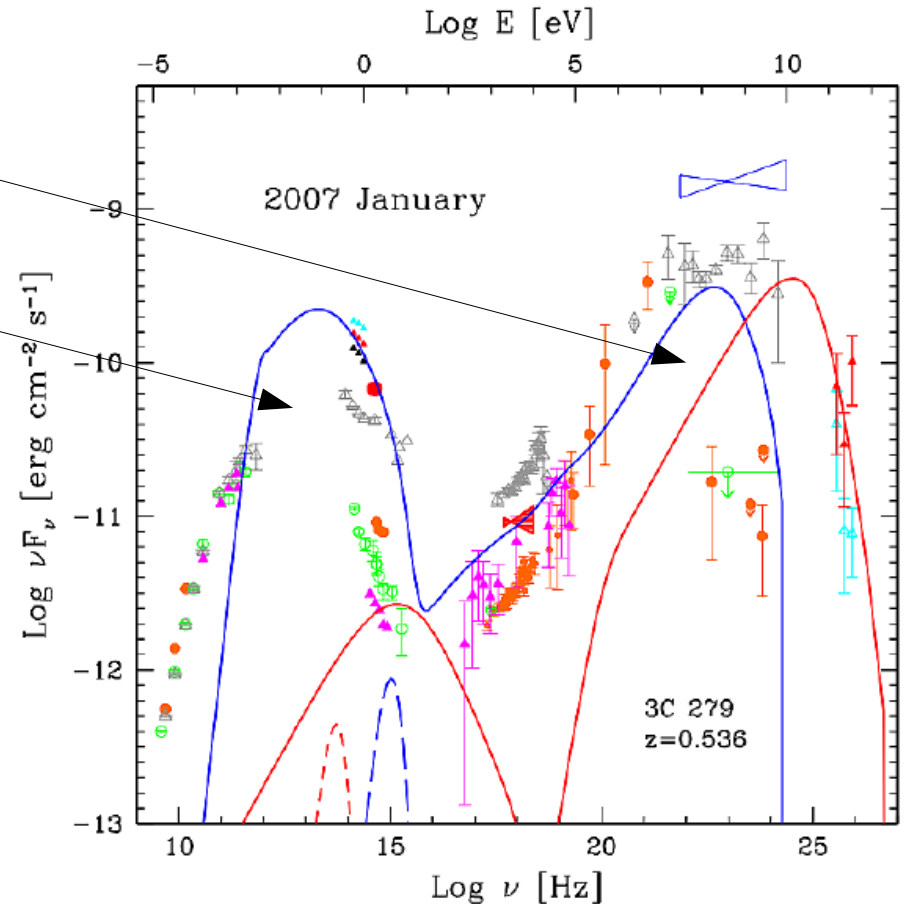
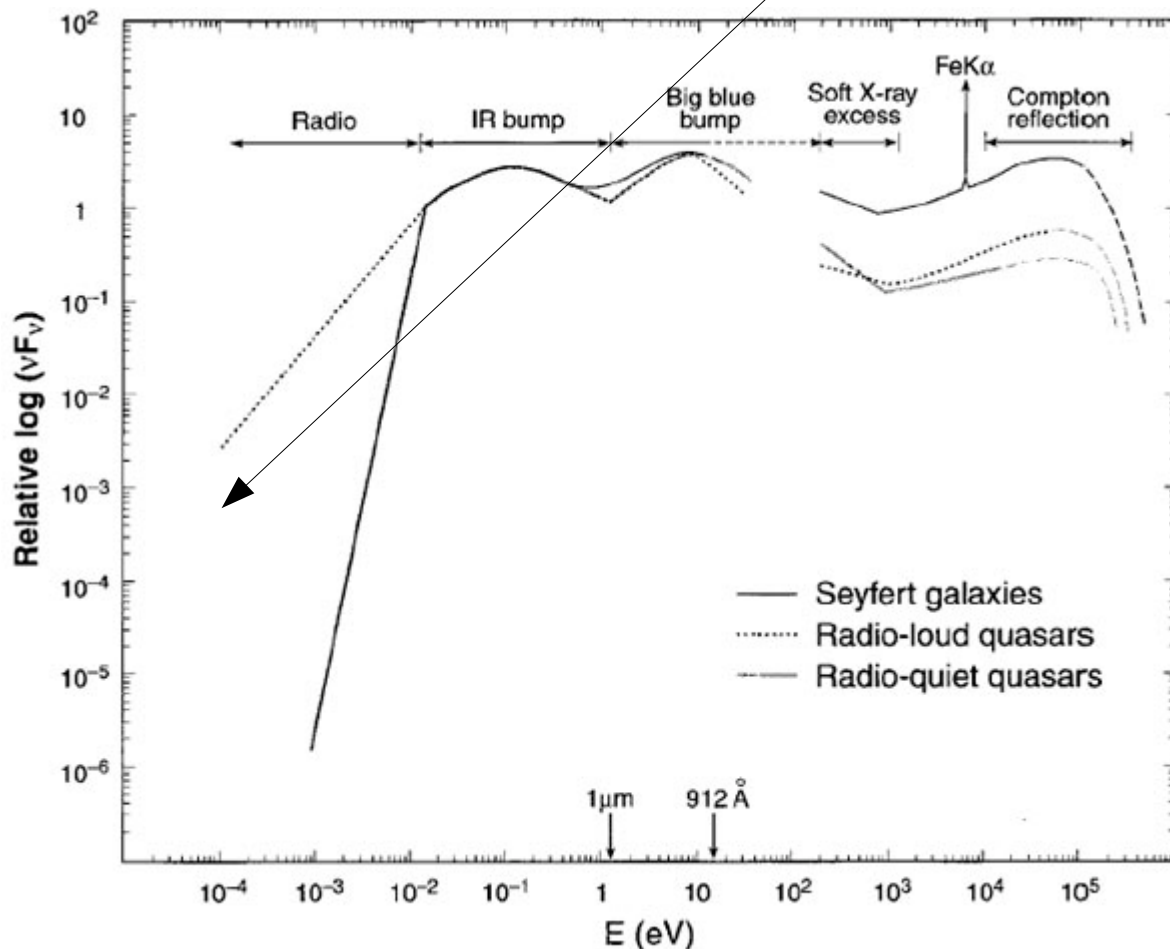


Figure 3: January 16<sup>th</sup>, 2007 SED of 3C 279 (red symbols, like in Figure 2, but red triangles at infrared are from REM). The two lines show the emission from inside (blue) and outside (red) the broad line region. Dashed lines as in Figure 2.

From Berger et al. (2011), here data from 2006.

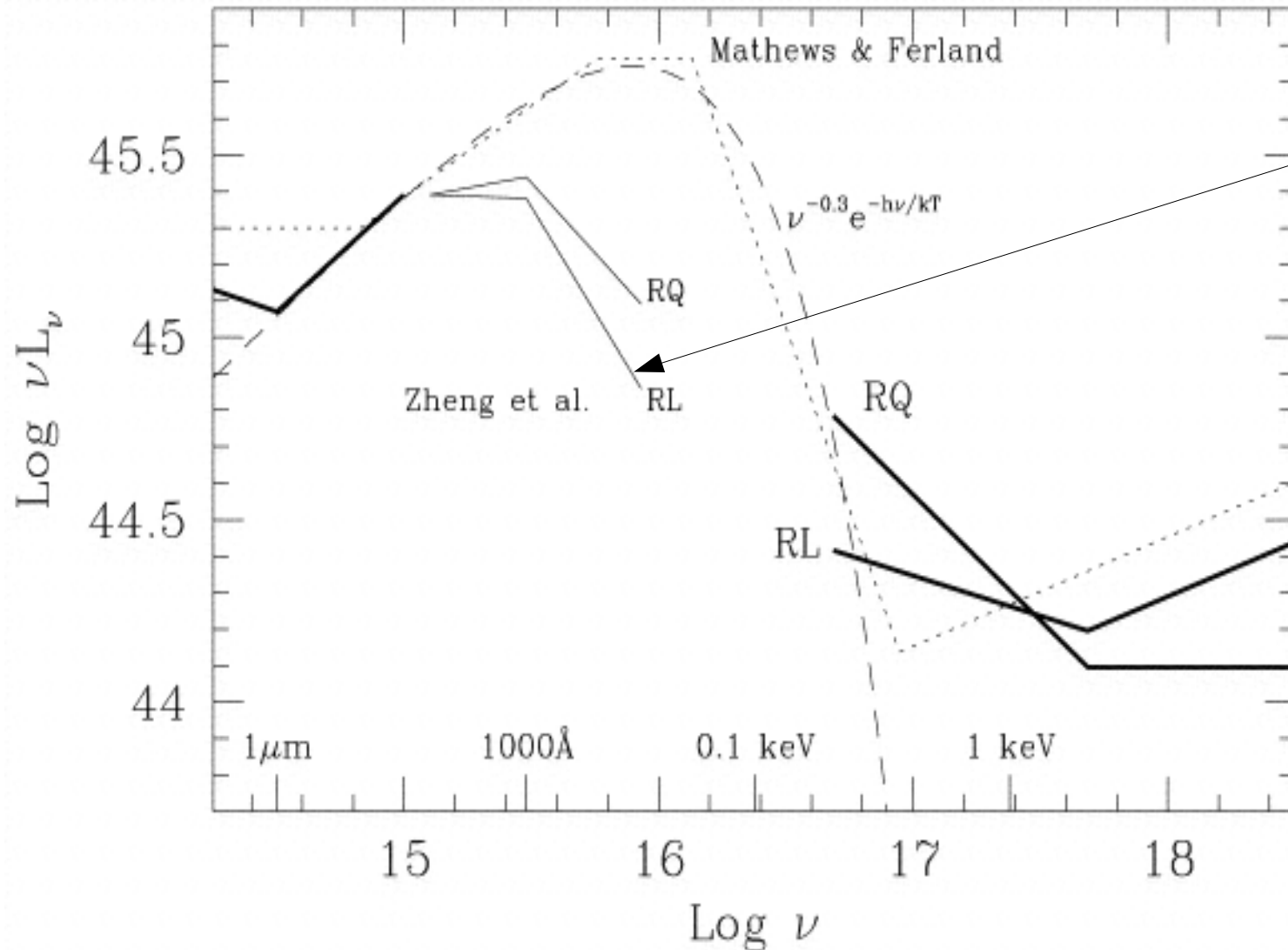
## 4. Jetted sources

If the jet is not oriented towards us, we see the broad spectrum which is actually very similar in RL and RQ quasars. The difference is by orders of magnitude in radio band but this band does not seem that important in the overall energy budget.



## 4. Jetted sources

If the jet is not oriented towards us, we see the broad spectrum which is actually very similar in RL and RQ quasars. Enlarged version of the UV/X-ray part shows redder spectra in RL sources



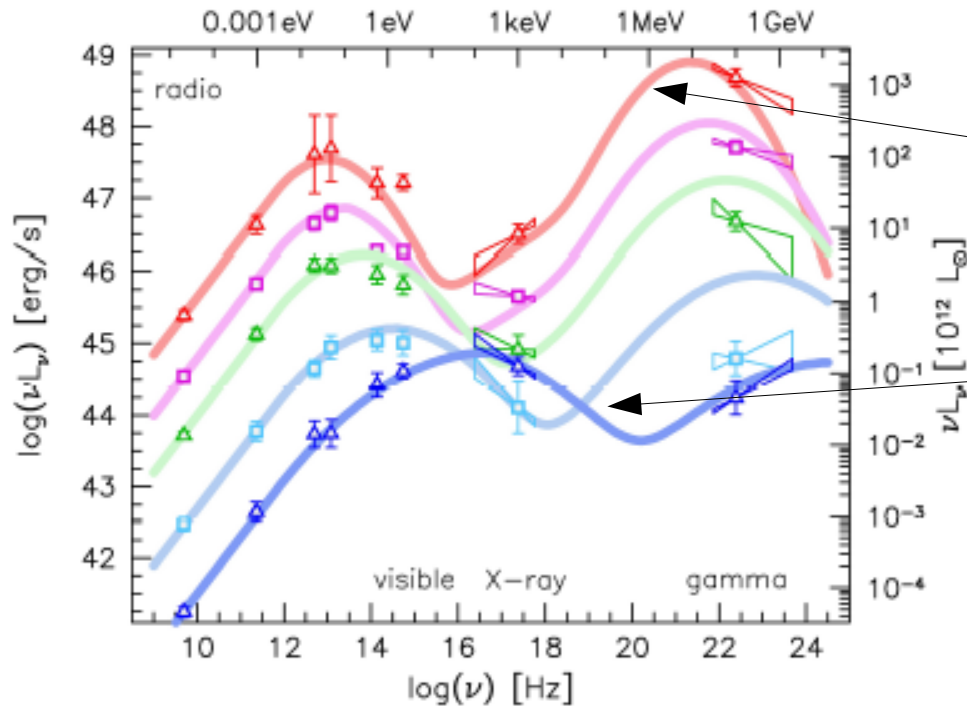
in the optical band, lower contribution of the Comptonization to the disk emission or actually some drain of energy from the disk close to to ISCO. On the other hand, the X-ray spectrum is harder, some contribution from the jet is likely seen there.

Laor et al. (1997) composite spectrum of RL and RQ quasars.



## 4. Jetted sources

In blazars we possibly see a **blazar sequence**, with fainter object peaks moving towards higher energies. This is most likely related not just to the black hole mass but also to Eddington ratio.



Sources like BL Lac itself rarely show the emission lines even if they are in the low state.

Sources along this sequence are classified as Flat Spectrum Radio Quasars (FSRQ) – they have strong emission lines in low state and BL Lacs which lack strong lines.

When the jet is not directed towards us but is almost in the plane of the sky FSRQ and BL Lacs find correspondence in the FR II/FR I division.

*Blandford et al. (2018) after Fossati et al. (1998)*

This division most likely is connected with the presence of the cold Keplerian disk close to ISCO (FSRQ, FR II), or the replacement of the inner cold disk with a hot inner flow (ADAF, RIAF etc.) following the trend with  $L/L_{\text{Edd}}$  as in radio-quiet objects.

## 4. Jetted sources

The division of radio-galaxies into Fanaroff-Rayleigh I (FRI) and II was introduced already in 1974.

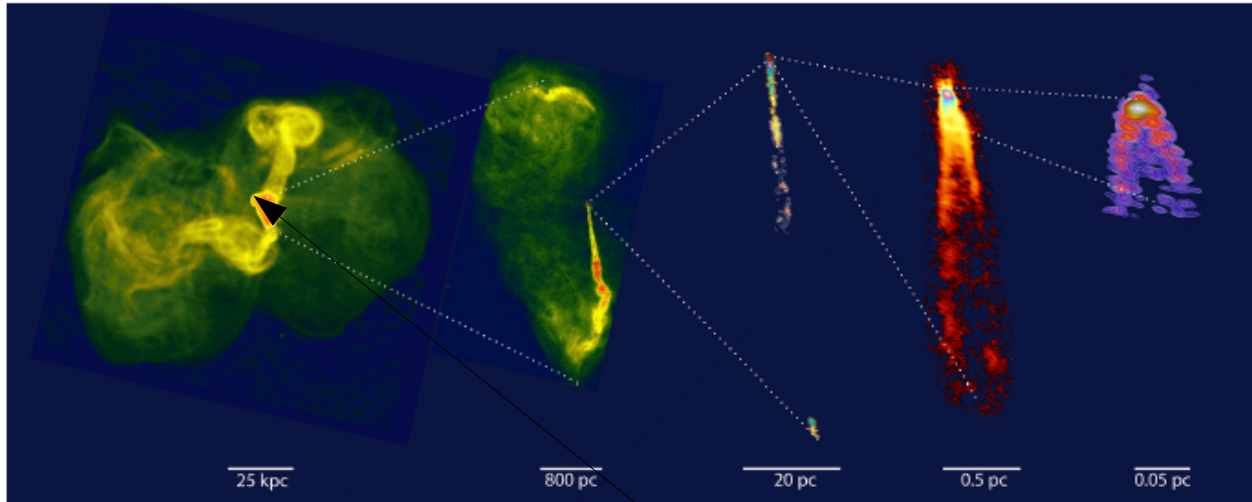


**Figure 1**

Montage of the FR-I radio galaxy M87, on scales from the outer lobes to near the black hole.



**Figure 4**

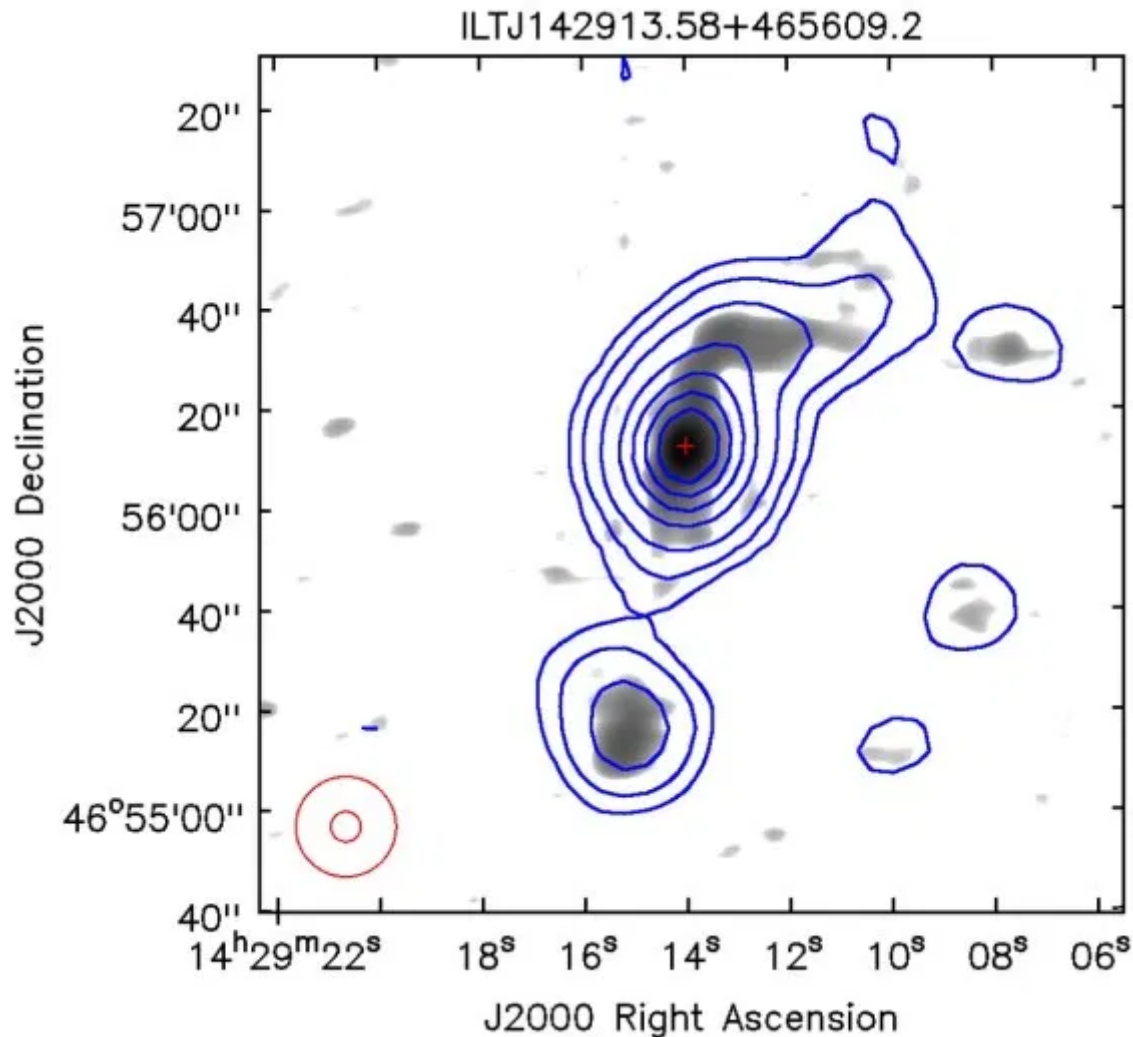
Comparison of radio (red), X-ray (blue), and optical images of the Cygnus A FR-II radio galaxy

FRI shows a bright core and relatively faint lobes while FR II has faint core but very bright lobes with hot spots.

*Figures from Blandford et al. (2018).*

## 4. Jetted sources

Jetted sources give interesting constraints on the duration of the activity episodes. The hot spot moves with the speed of order of 0.1 – 0.5 light speed (jet is relativistic, but there it almost stops !). Kuźmicz et al. (2018) presented an updated catalog of 349 gigantic radio galaxies with sizes between 0.7 Mpc and 7.7 Mpc. Such an outburst has to last at least about 10 million years in a continuous way, without disrupting accretion disk instabilities.



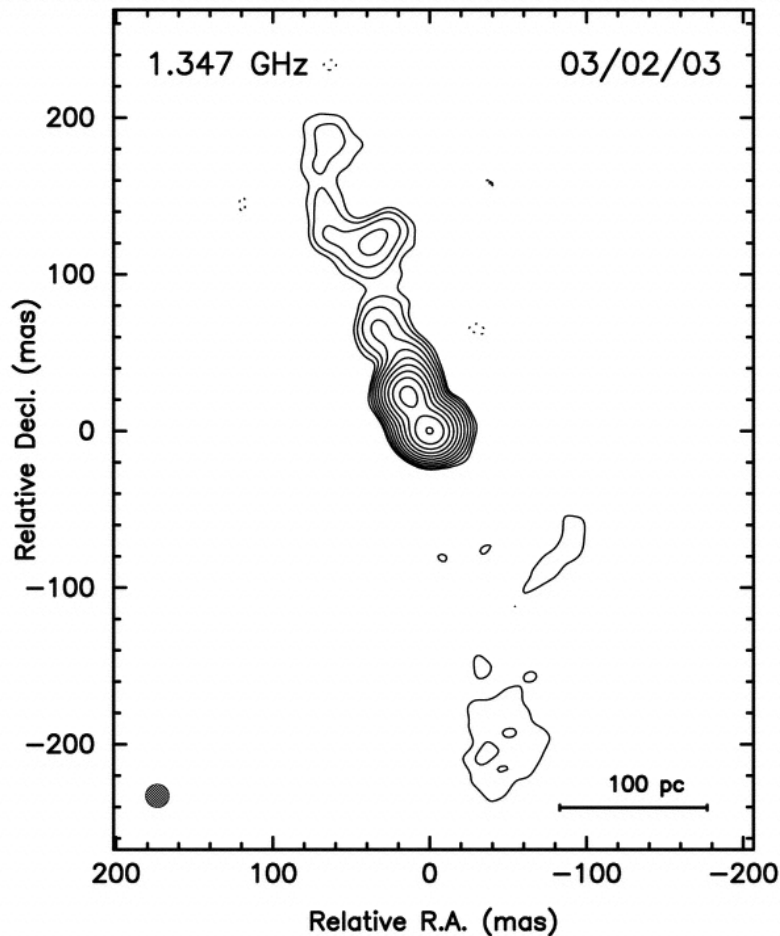
*Giant radio galaxy from LOFAR survey  
(Dabhade et al. 2019)*

## 4. Jetted sources

On the other hand, numerous radio sources never grow large (age below 100 000 years), and if they are young this phase should be statistically rarely seen unless

- These jets become 'frustrated' - stopped by the dense interstellar medium
- Radiation pressure instability operates, and interrupts the strong activity stage in this sources, later the source starts again but always stops soon, repeating the apparently young stage ad infinitum.

Subclass of radio galaxies is classified as Compact Symmetric Objects (CSO), and their jets are small, much smaller than FR I or FR II.

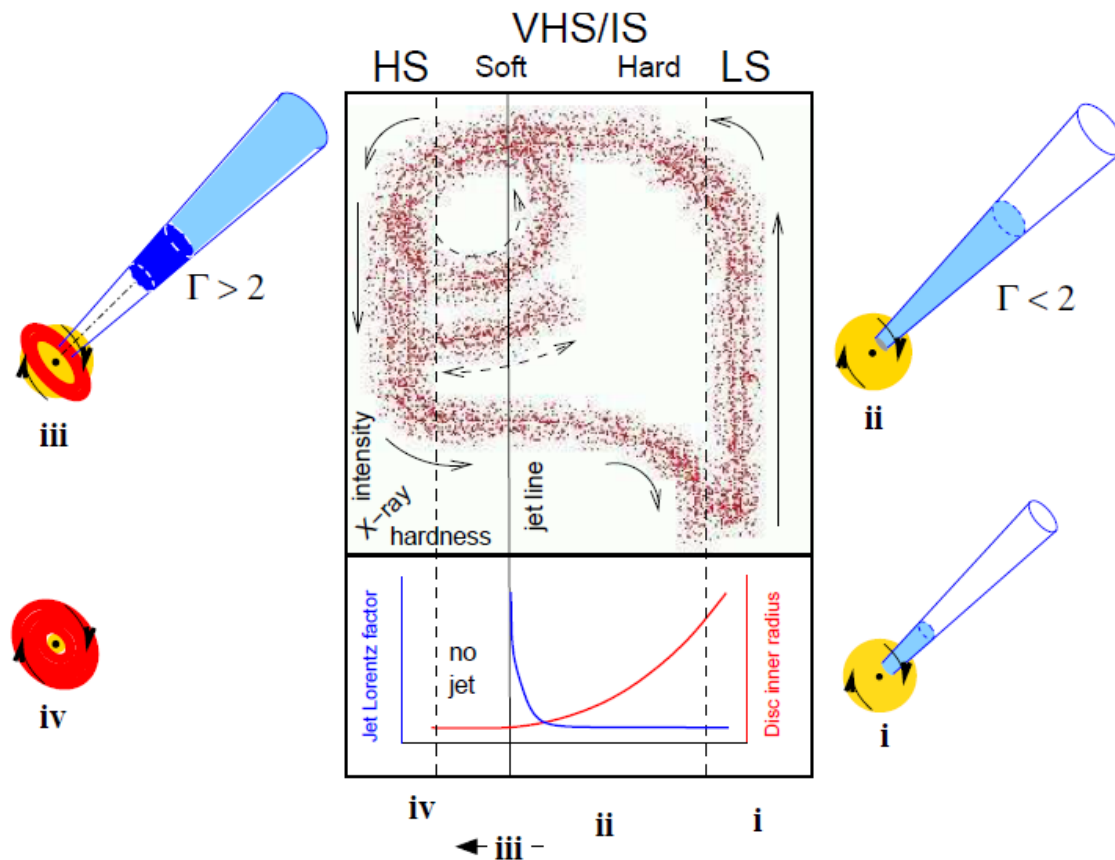


*VLBA image of the CSO 0402+379 source from Maness et al. (2003); this one has an additional faint large kpc structure seen in VLA data...*

## 4. Jetted sources

Only about 10% of AGN are classified as radio-loud. Why is that?

- Evolutionary stage ?
- Black hole spin?
- External magnetic field ?



In Galactic sources (X-ray novae) we had this diagram which showed that the same source can have a jet and can have no jet.

We do not have a similar diagram since (i) we have a systematic difference in accretion disk temperature and corresponding wavelength range (UV/X-ray) (ii) we cannot follow the evolution since this takes millions of years (iii) statistical approach is additionally messed up by the differences between black hole masses in different sources (from  $10^5 M_{\odot}$  to  $10^{10} M_{\odot}$ ).

*Schematic representation of the X-ray nova from Remillard & McClintock (2006) after Fender et al. (2004).*



## 5. Radio-quiet sources

Radio-quiet galaxies are classified mostly according to the shape of their emission lines and we will concentrate here on this issue (but this works also for radiogalaxies)



**Seyfert 1 galaxies and most quasars**



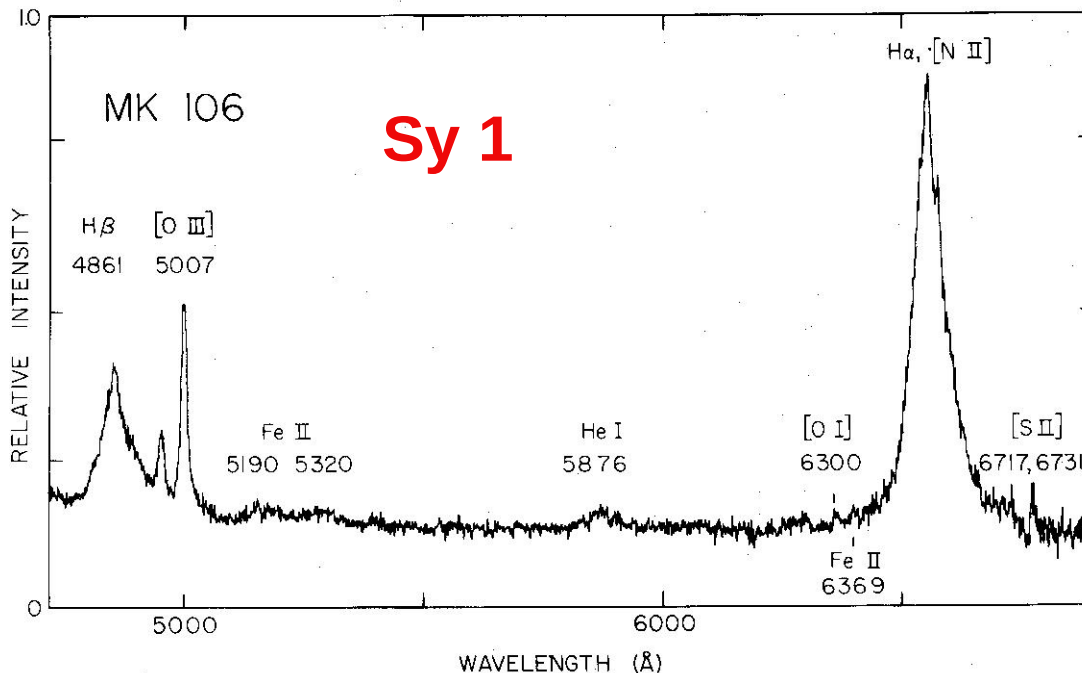
**Seyfert 2 galaxies and rare quasars**



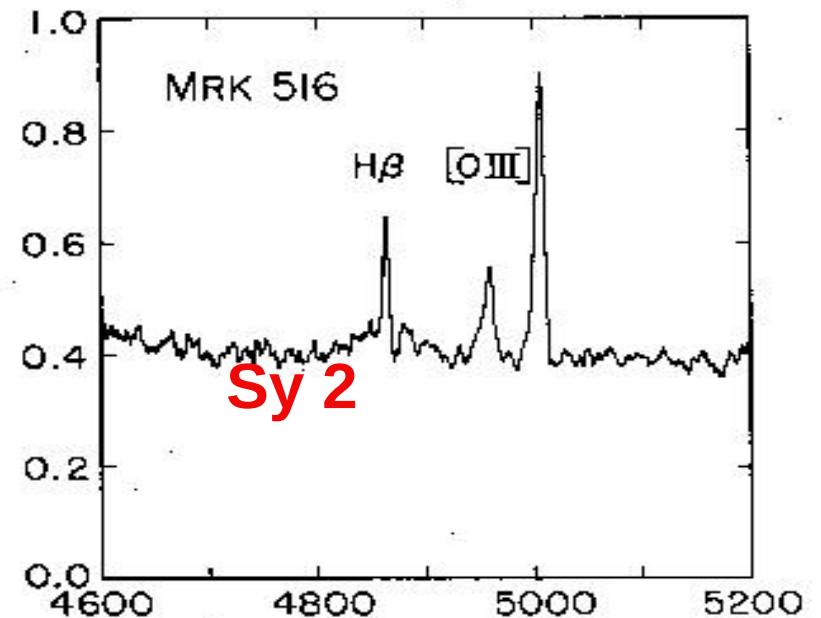
**LINERS**

The Sy1/Sy2 classification was introduced by Khachikian & Weedman (1974). The physics underlying this classification is a difficult combination of the orientation effect and the change of the Eddington ratio.

Here Hbeta much broader than OIII (type 1)



Here Hbeta is the same as OIII (type 2)



# 5. Radio-quiet sources

## 5.1 Narrow Line Region (BLR) and Broad Line Region (NLR)

The broad emission lines have the kinematic width of 2000 – 20 000 km/s.

The narrow emission lines have the kinematic width about a few hundred km/s.

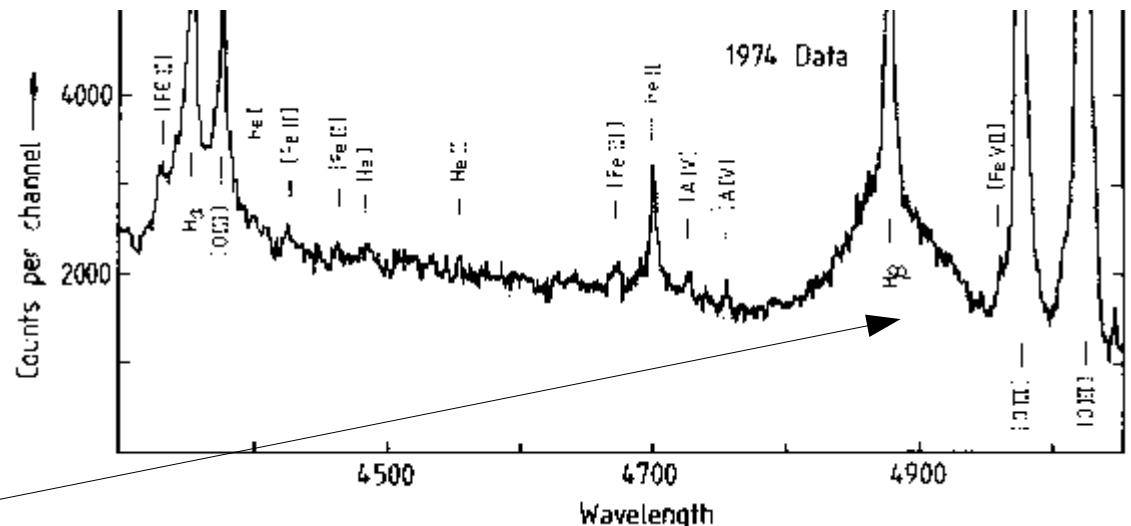
Some lines are always narrow, for example [OIII] 5007 A which is a forbidden line, form only in low density medium far away from the nucleus (tens to hundreds of pc).

Hbeta line can be broad, can be narrow since permitted lines form is a broad range of possible densities.

### 5.1 Seyfert 1 galaxies and type 1 (majority) of quasars

The most popular Seyfert galaxies have a complex shape of the Hbeta line. It consists of a narrow core and broad wings. The presence of the broad wings of permitted lines is the signature of being type 1 object.

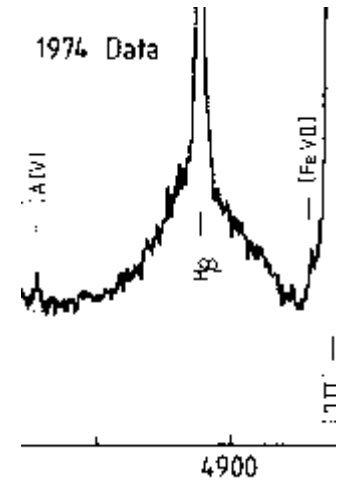
This complex line shape implies the presence of two distinct emission regions.



Spectrum of NGC 4151 in 1974 (from <https://www.ing.iac.es/PR/SH/SH8485/ngc4151.html>)

## 5. Radio-quiet sources

If the line width implies the Keplerian velocity around the nucleus, it looks like type 1 objects have strongly stratified line emitting region.



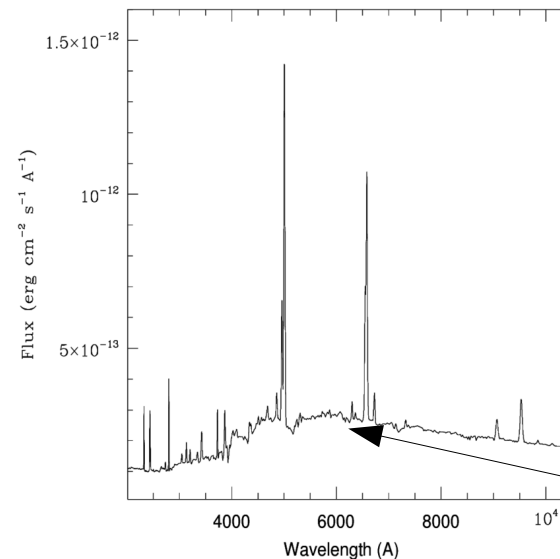
The presence of the gap is explained by the presence of the dust at a distance where the cloud temperature falls below some 1500 K (Netzer & Laor 1993) since there the gas efficiently compete for photons and the Hbeta line production suddenly drops down (but recovers later on).

The component from the NLR has roughly the same width as the forbidden lines.

### 5.2 Seyfert 2 galaxies and type 2 (rare) quasars

In this sources we do not have the broad component. Thus:

- Either there is no BLR in type 2 object
- Or BLR is hidden from our view



*Spectrum of NGC 1068 (Sy 2) from Pritzkal et al. (2011); Hbeta is narrow and weak.*

# 5. Radio-quiet sources

## 5.2 Seyfert 2 galaxies and type 2 (rare) quasars

The major break though came with the polarization observations done by Antonucci & Miller (1985) of NGC 1068.

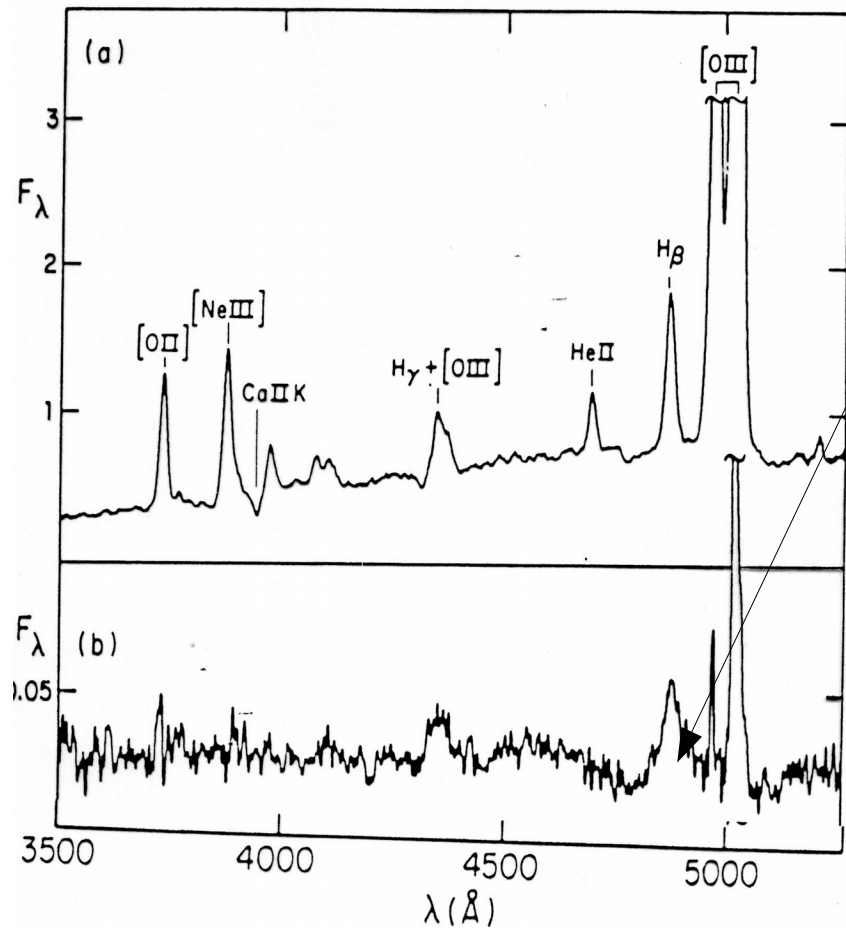
In unpolarized light they saw narrow and faint Hbeta line, since the source was classified as Sy 2 galaxy.

But in polarized light the Hbeta line appeared broad, like in typical Sy 1.

Thus this observation showed that BLR actually exist in this source, but it is hidden from our line of sight.

They interpreted the situation geometrically as this.

In polarized light we see predominantly just the scattered emission, so the direct NLR contribution is then fainter,



Material from Antonucci & Miller (1985).

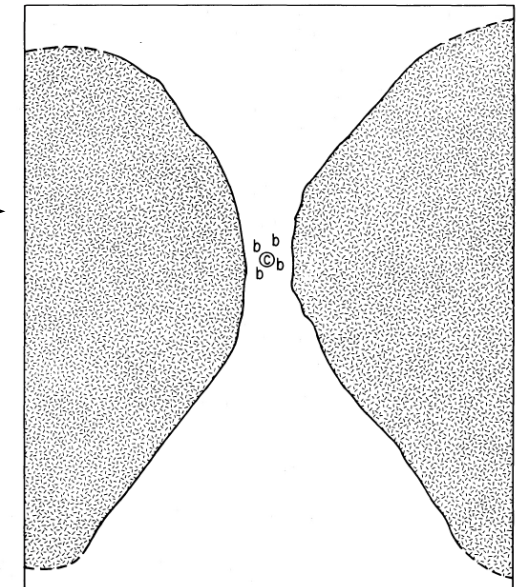
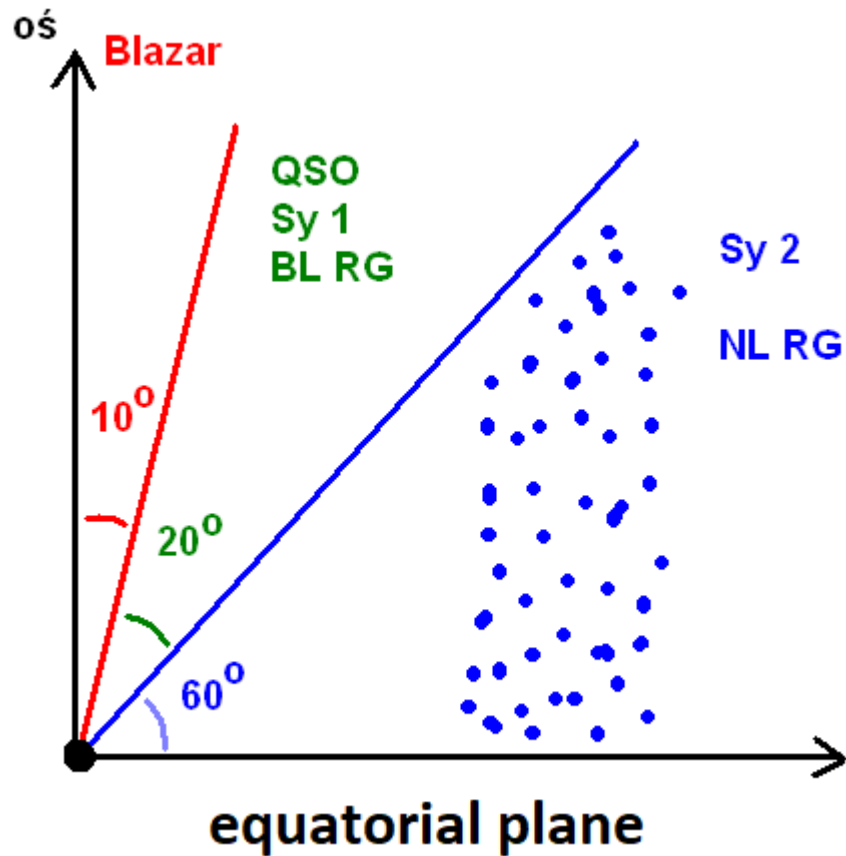
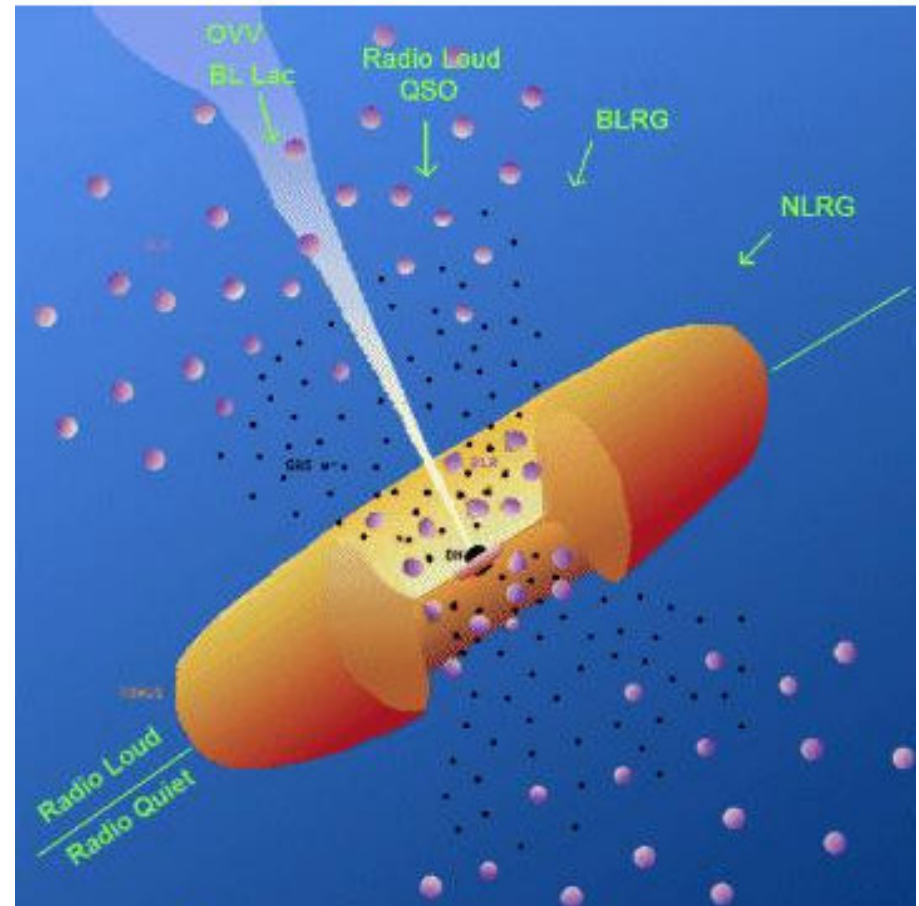


FIG. 5.—Cutaway drawing of a continuum source surrounded by a geometrically and optically thick disk. Only photons traveling out along the polar directions can scatter into the line of sight. We would observe a high polarization in the plane perpendicular to the symmetry axis, which we presume to be the radio structure axis.

## 6. Classification scheme according to orientation



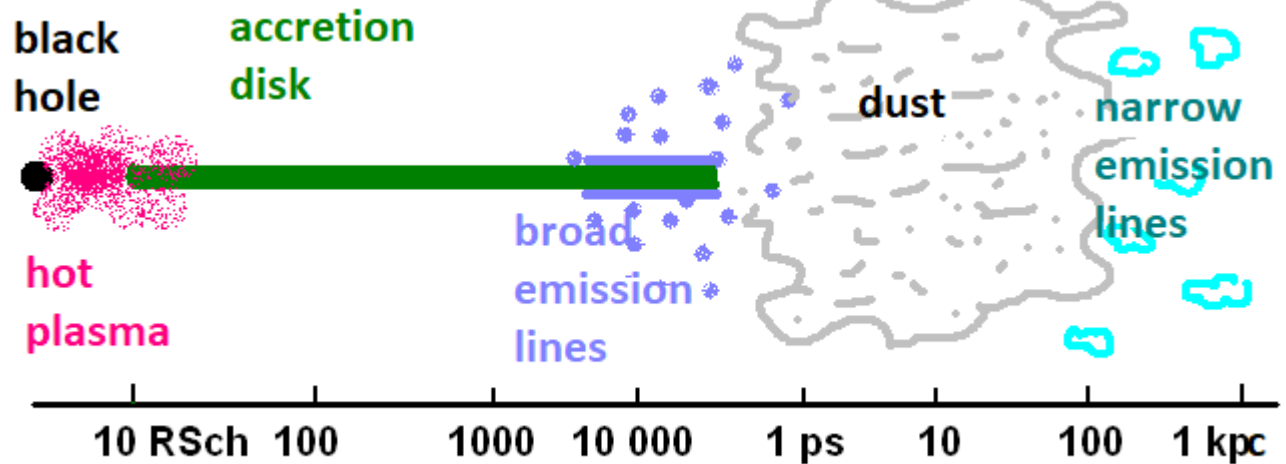
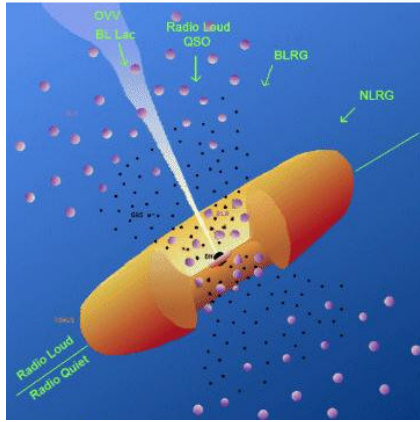
The orientation effect offers a universal scheme for AGN. The low numbers of type 2 quasars are likely due to the selection effect.



*A version of classical picture from Urry & Padovani (1996).*



## 6. Classification scheme according to orientation



The dusty torus must be clumpy. The BLR is also likely clumpy although continuous wind models are considered.

The onset of the BLR is perhaps determined by the presence of the dust in the accretion disk atmosphere (Czerny & Hryniewicz 2011), while the outer radius is set by the dusty/molecular torus, where dust can survive even under irradiation from the nucleus (Netzer & Laor 1993).

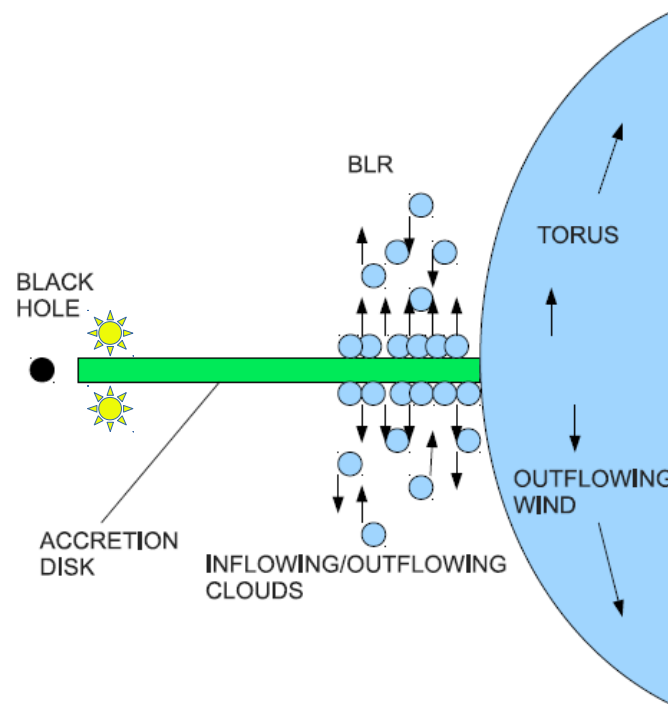
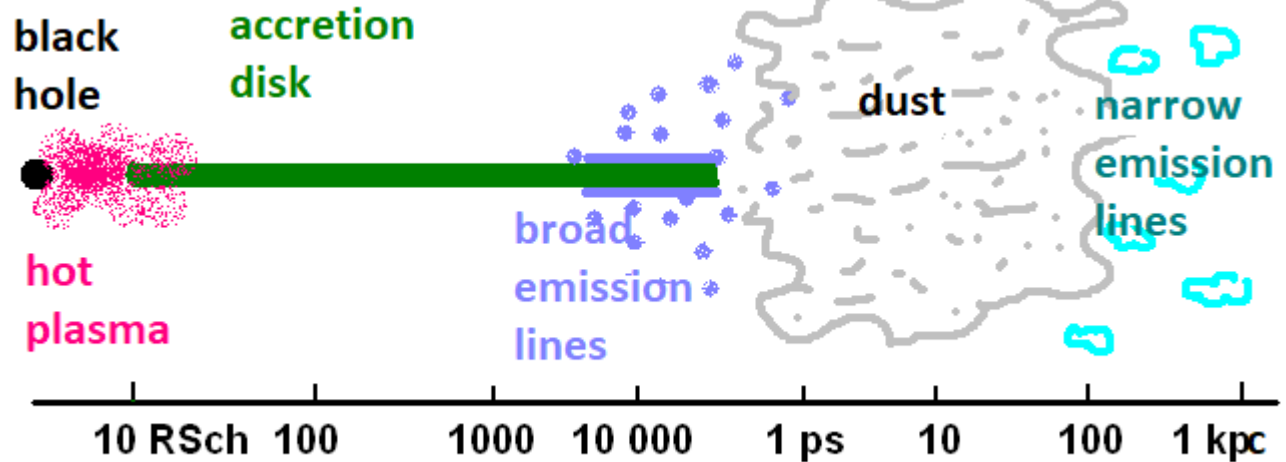
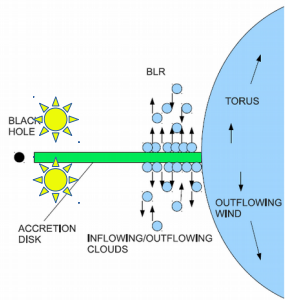
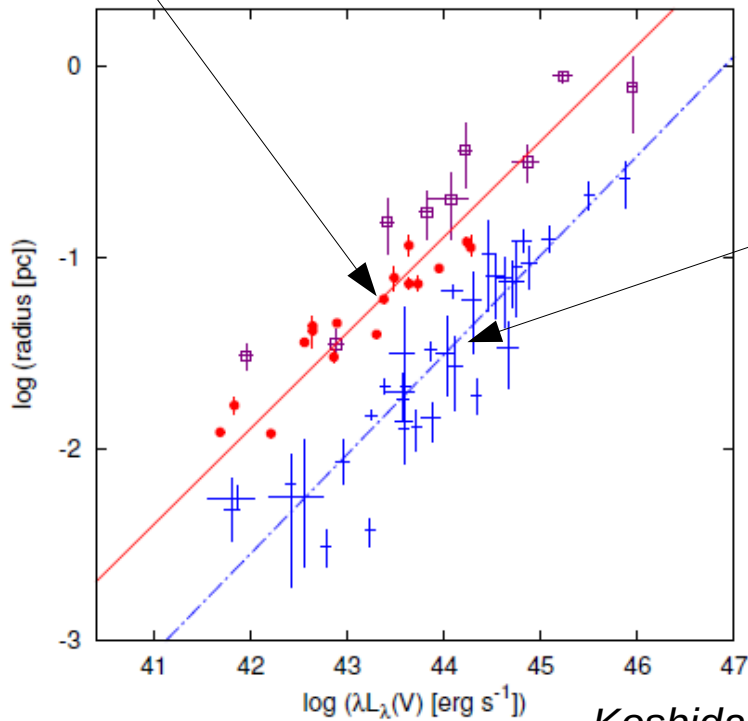


Illustration of our FRADO model (Failed Radiatively Accelerated Dusty Outflow) of BLR.

## 6. Classification scheme according to orientation



Reverberation mapping (time delay measurements) allow to measure the size of the BLR and the inner radius of the torus.

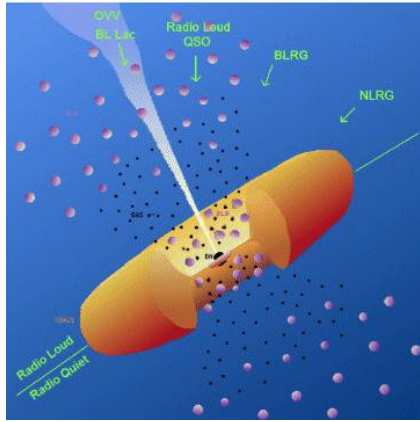


This radius-luminosity relation is also a key to massive black hole mass measurements in AGN. We then use the virial relation:

$$M = f_{\text{vir}} \frac{v^2 R_{\text{BLR}}}{G}$$

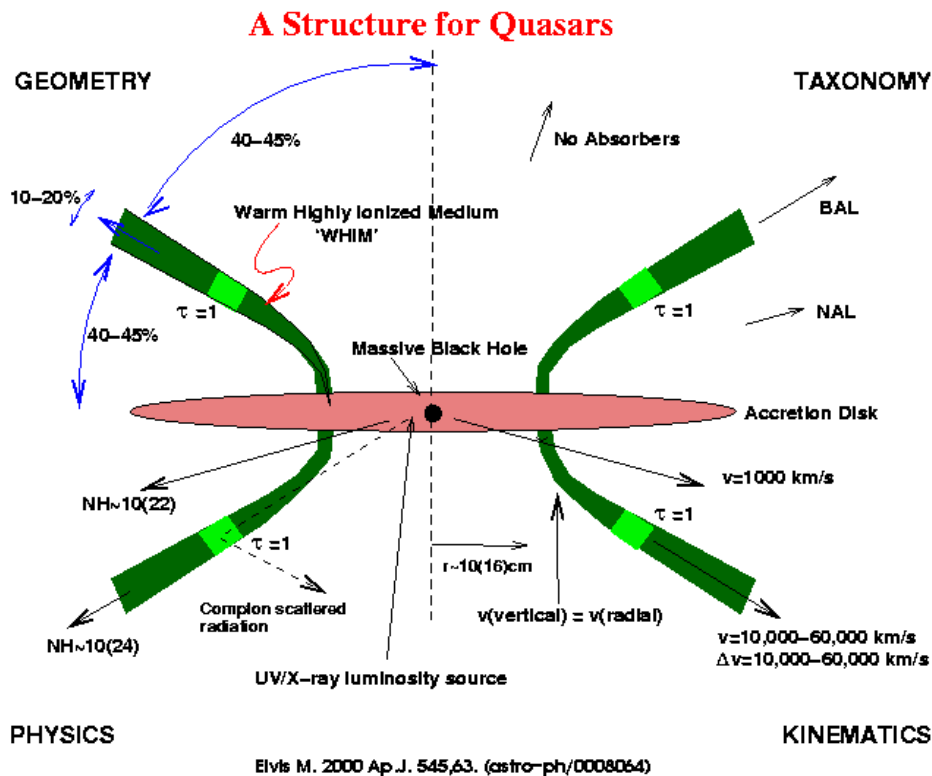
supplementing FWHM of the line for velocity, and using R-L relation to estimate the radius.

## 6. Classification scheme according to orientation



The exact nature of the dusty torus is not known but it cannot be a static torus in the gravitational field of a black hole, it must be also some form of a wind. Perhaps a fraction of the inflow is actually reversed into outflow under the radiation pressure.

It also can originate from the cold Keplerian disk, but the disk structure at such distances is not well specified (self-gravity!), the timescales of such disk are too long for the duration of an active phase.



This idea explains the additional features seen in a fraction of quasars (Broad Absorption Lines – BAL; Narrow Absorption Lines – NAL, and Warm Absorber).

This can be set by extensive multiwavelength reverberation mapping.

## 7. Beyond the universal picture

AGN are actually classified more carefully as:

**Radio load/radio quiet:**  $\log (F(5 \text{ GHz})/F(B)) > 1$

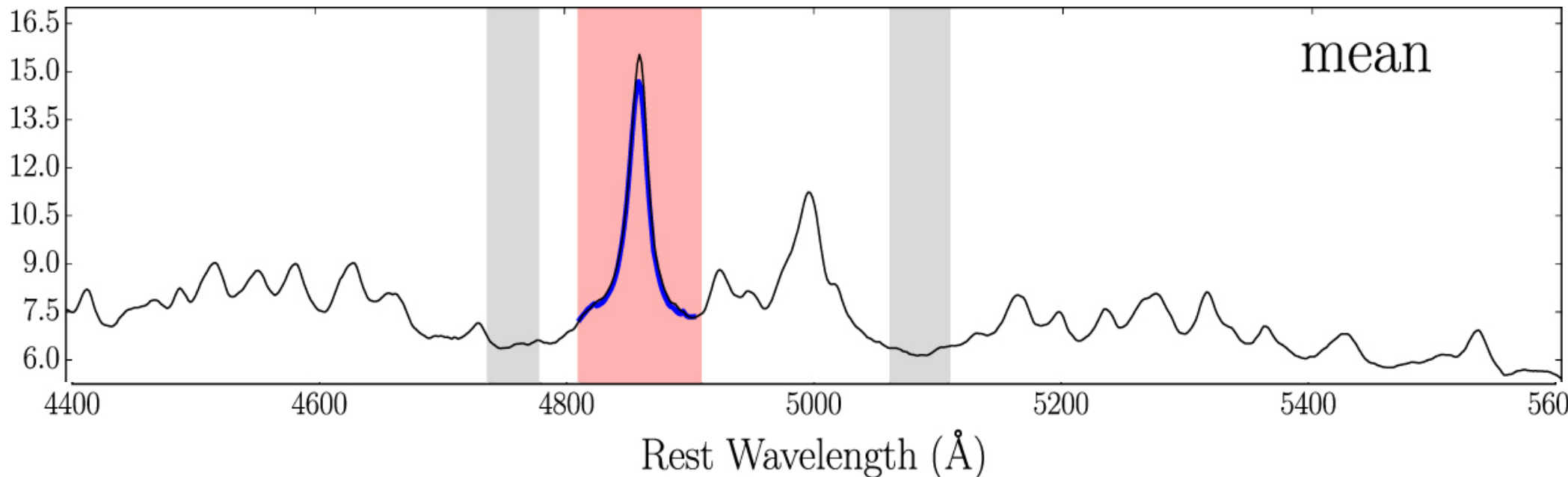
**QSO/Seyfert :** absolute luminosity in B band  $M_B < -23$

**Sy 1, Sy 1.2, Sy 1.5, Sy 1.8, Sy 1.9, Sy 2:**  $L(\text{broad H}\beta)/L([\text{OIII}]\lambda 5007)$  above 5, 5-2, 2 – 1/3, below 1/3 but with traces in  $\text{H}\alpha$ , no broad component in Hbeta but seen in  $\text{H}\alpha$ , nothing even in  $\text{H}\alpha$ . But apart from this classification we also have Narrow Line Seyfert 1 galaxies and type A quasars.

**7.1 Narrow Line Seyfert 1 galaxies** have line somewhat broader than Sy2 but narrower than classical Sy1. Classification was introduced by Osterbrook & Pogge (1985).

The definition:

$[\text{OIII}]\lambda 5007$  emission ( $\text{FWHM}_{\text{H}\beta} < 2000 \text{ km/s}$  and  $[\text{OIII}]/\text{H}\beta_{\text{tot}} < 3$ ;



*I Zw 1 spectrum (Huang et al. 2019)*

## 7. Beyond the universal picture

In those sources the torus is not located along the line of sight, the lines are intrinsically narrow.

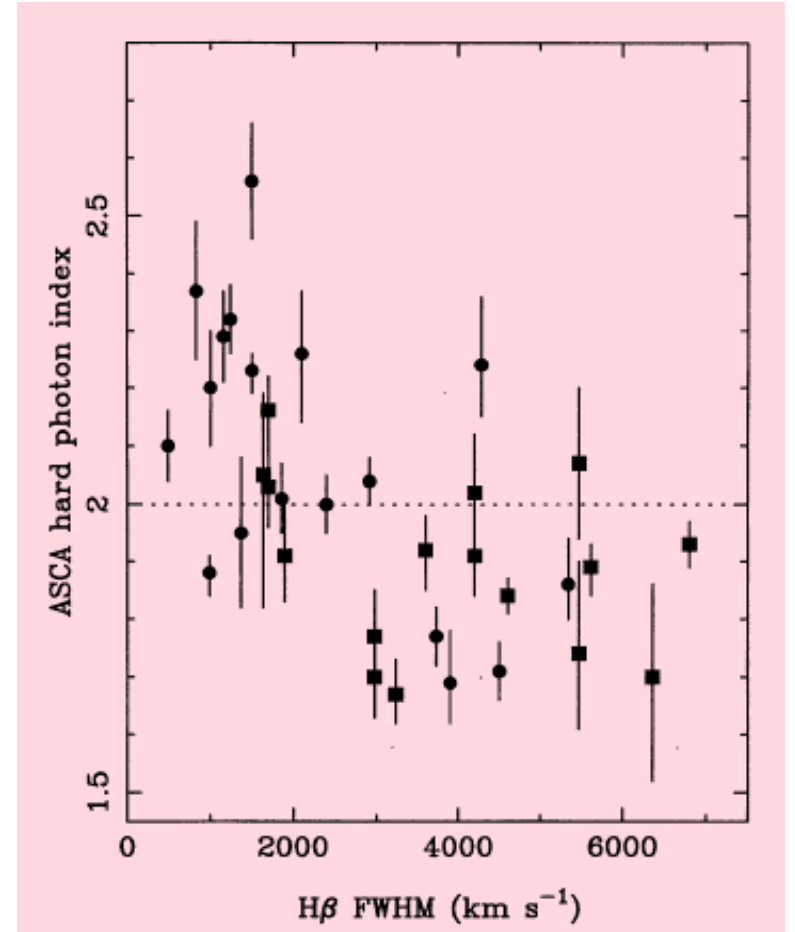
There is a number of arguments that these sources are high Eddington ratio sources.

First, in general these sources show a different slope of the X-ray spectrum, resembling Very High State in Galactic sources.

Second, high source luminosity causes the BLR to recede (closer in the material is too highly ionized to emit H $\beta$  line), and the lines become narrower.

Third, apparently there is no gap between the NLR and BLR in these sources (simple line shape). We were able to model it using high density clouds appropriate for high Eddington ratios (Adhikari et al. 2016); dust in high density cloud cannot compete with gas for photons, unlike in Netzer & Laor (1993).

The limit between Sy1 and NLS1 apparently depends on the black hole mass. It is at 2000 km/s for a  $10^7$  Ms, and about 4000 km/s for  $10^9$  Ms (division into type A and type B quasars, Sulentic et al. 2000).

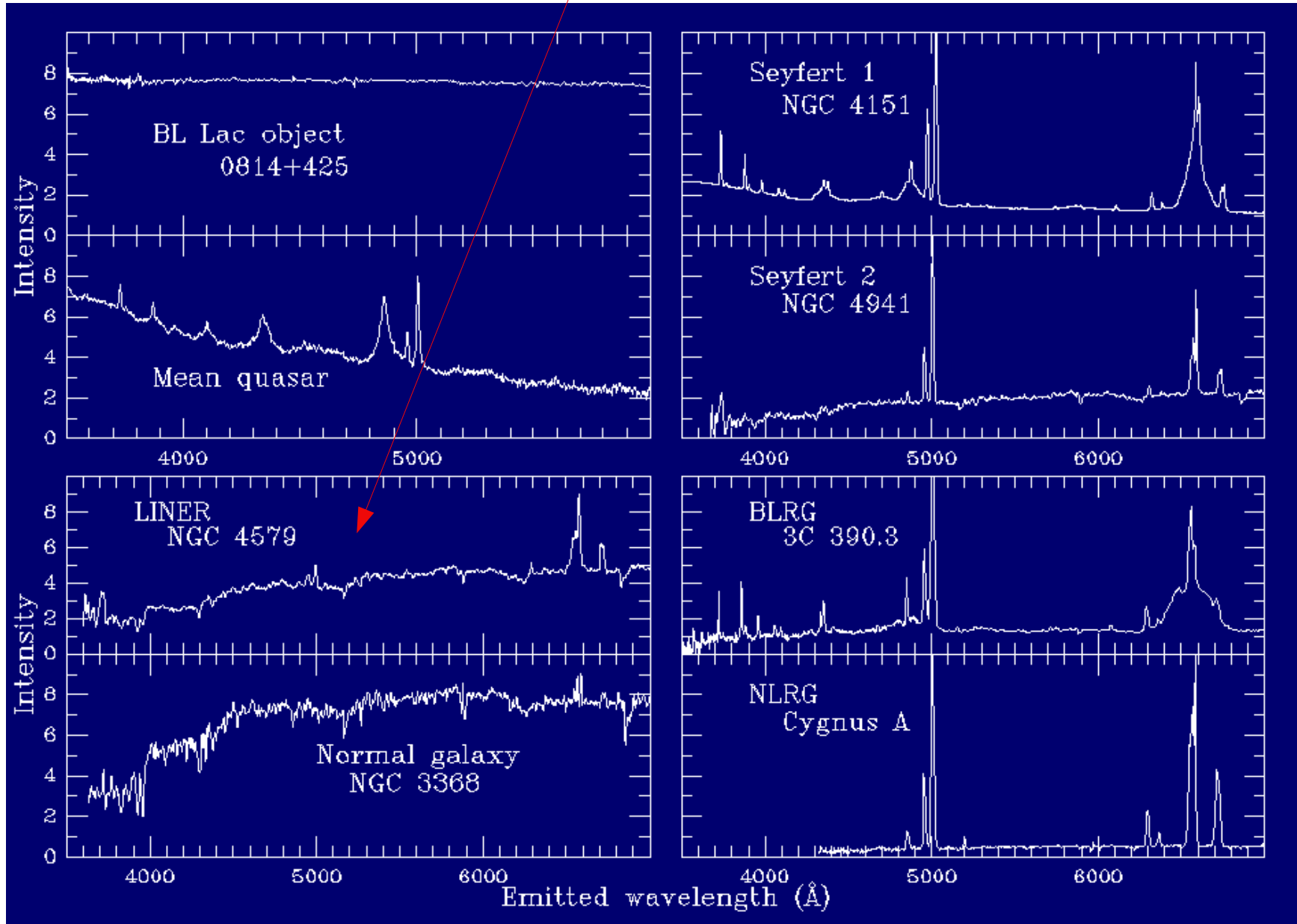


*Dependence of the X-ray slope of the spectrum on the width H $\beta$  line, Brandt et al. (1997)*



## 7. Beyond the universal picture

**LINERS** (Low-Ionization Nuclear Emission Line Region) – a class introduced by Timothy Heckman in 1980. About 30 % of all galaxies belong to this class, their activity is weak, and they most likely correspond to very low Eddington ratio flow.



## 7. Beyond the universal picture

**Sy 2 Hidden BLR/true Sy 2** Antonucci & Miller (1985) solved the problem for NGC 1068 which is actually a very bright AGN with high inclination. In many Sy 2 the BLR was discovered in polarized light but in many no such component is seen in the data.

The question remains whether the objects which do not show the hidden BLR indeed do not have any, or the viewing angle is too low, dusty/molecular torus too thick and the amount of scatterers not enough to efficiently redirect a fraction of light towards the observer.

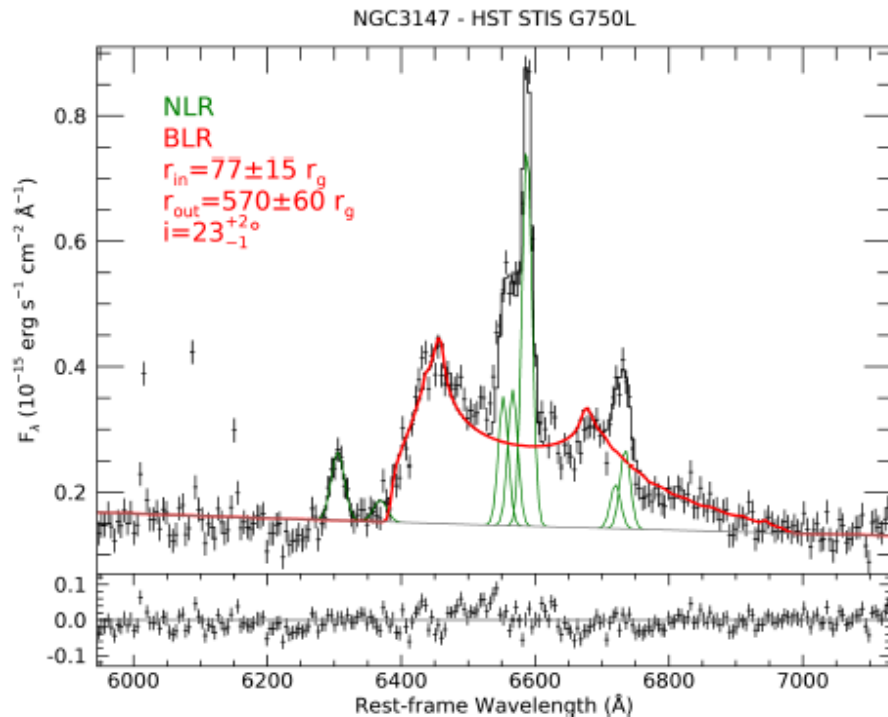


Figure 1. A remarkably prominent and very broad  $H\alpha$  line profile (in red) is revealed in the *HST* STIS G750L spectrum of NGC 3147, carrying the signature of a relativistic thin Keplerian disk, with an inner emitting radius of only  $77 r_g$ . Narrow lines from the NLR are in green, the continuum in grey. The fit residuals are shown in the bottom panel.

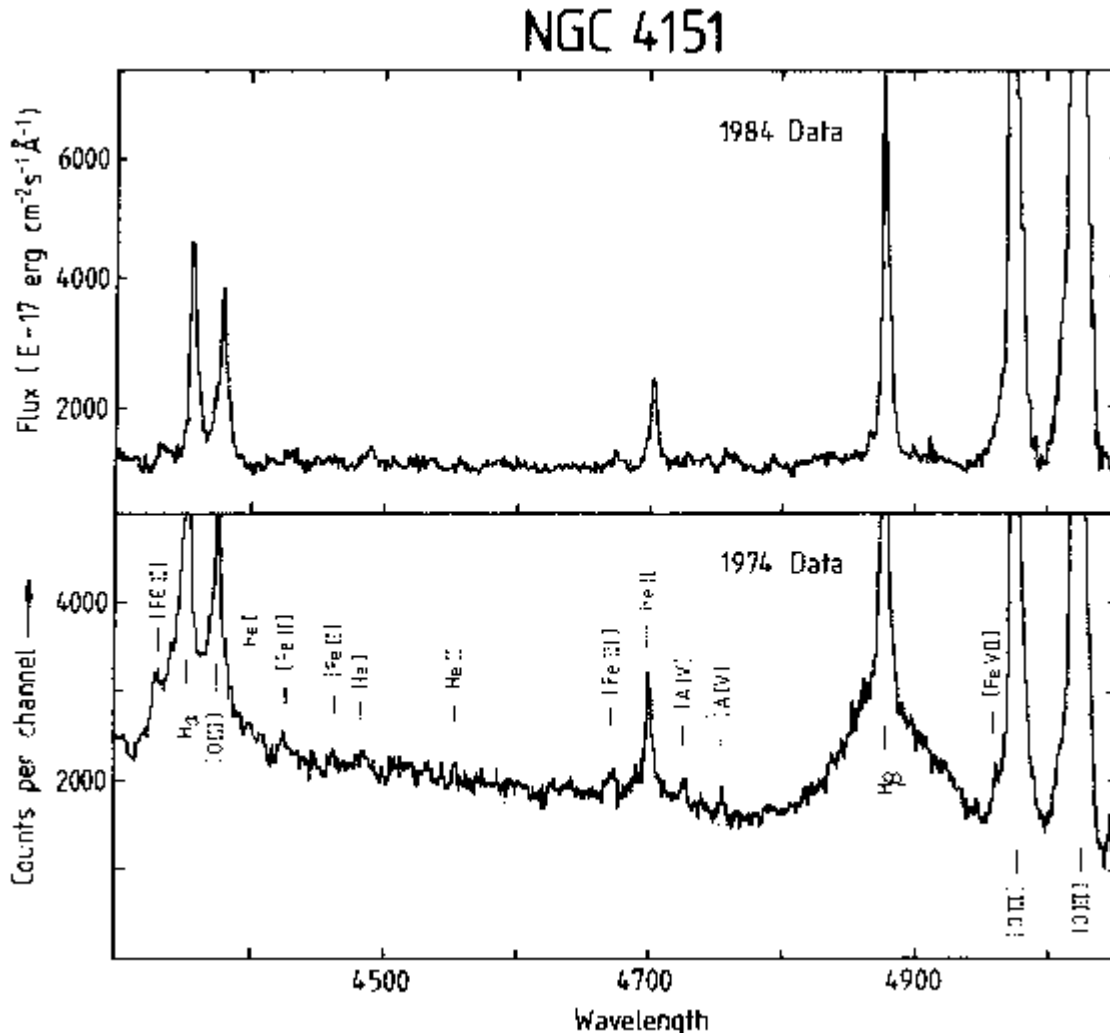
I would think that a combination of the two effects contributes, since with the decrease of the Eddington ratio the optically thick Keplerian disk likely recedes, and the BLR cannot form when the inner ADAF flow is too extended. M87 and Sgr A\* do not have a BLR for sure. But there are surprises.

Here we see narrow slit ( $0.1'' \times 0.1''$ ) *HST* spectrum of the best true Sy 2 candidate NGC 3147. The Eddington ratio is this source is  $10^{-4}$ , and the line is relativistically distorted, well modeled by emission from the accretion disk surface close to the black hole.

Bianchi et al. (2019).

## 8. Changing-look AGN

Even the most studied AGN show occasionally spectacular changes in their appearance. NGC 4151 looked like a Sy 1 in 1974 but in 1984 the broad component of H $\beta$  is barely seen.



Spectrum of NGC 4151 in 1974 (from <https://www.ing.iac.es/PR/SH/SH8485/ngc4151.html>)

Now several such examples are known. The change may be caused by obscuration, but it is more likely to be **intrinsic**, at least in some sources (after the episode of the BLR decrease, the size of the BLR shrinks in NGC 5548).

**The timescale of the change is too rapid for a viscous timescale at a few tens of  $R_{\text{Schw}}$ .**

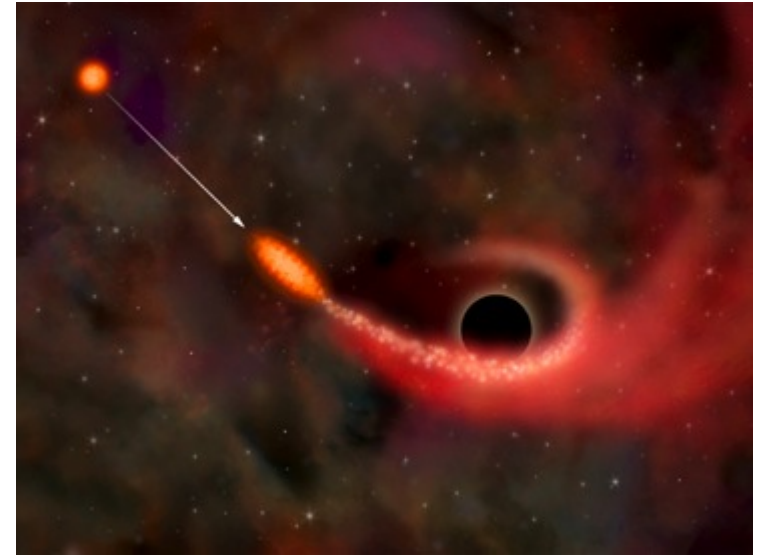
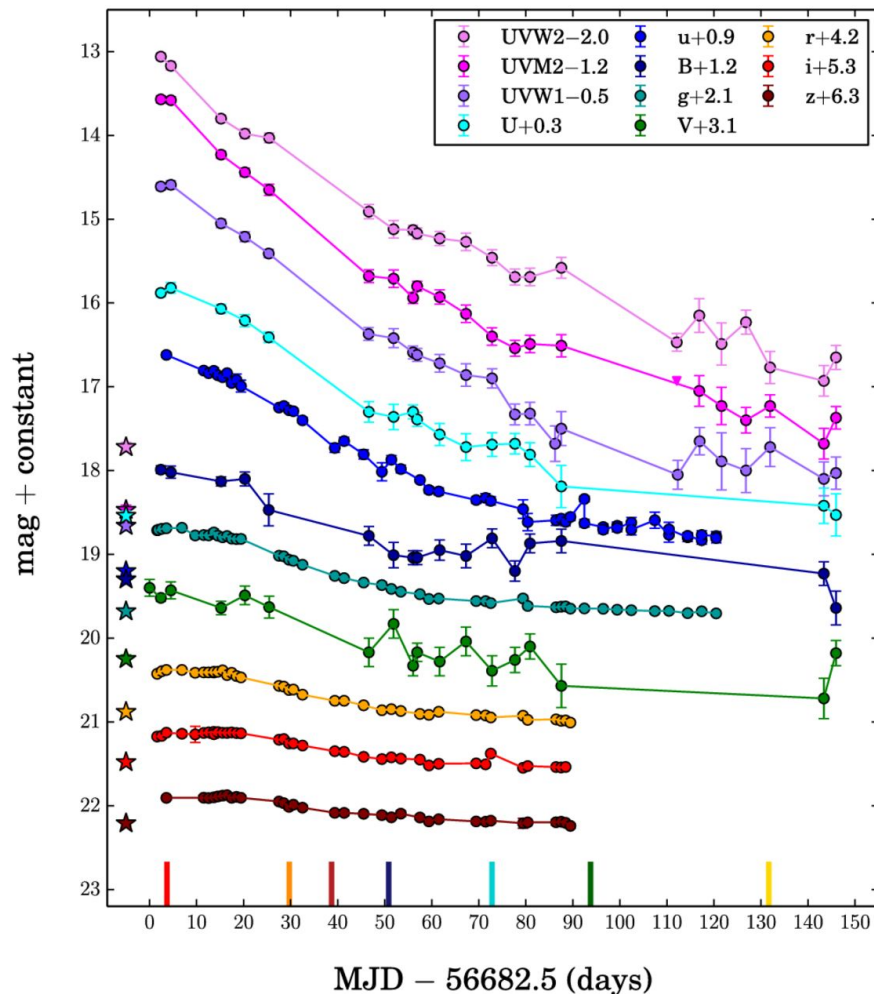
But the thermal timescale, and the inflow timescale for a hot coronal plasma is short enough to change the accretion rate close to a black hole efficiently.

We do not know the exact mechanism.

## 8. Tidal Disruption Events (TDE)

A star passing close to a massive black hole can be disrupted and activate otherwise dormant (only weakly accreting) nucleus. Several examples are known, as we discussed previously. They are being discovered during the searches for transient phenomena (e.g. ASAS-SN facility).

The active stage lasts for about a year.



*An artist's impression of the passage of a star close to a black hole, causing a Tidal Disruption Event (image courtesy CXO/NASA).*

They do not always look the same. It is possible that sometimes the star gets disrupted in the almost empty surrounding, but sometimes there are remnants of the accretion disk from the previous phase which affects the process.

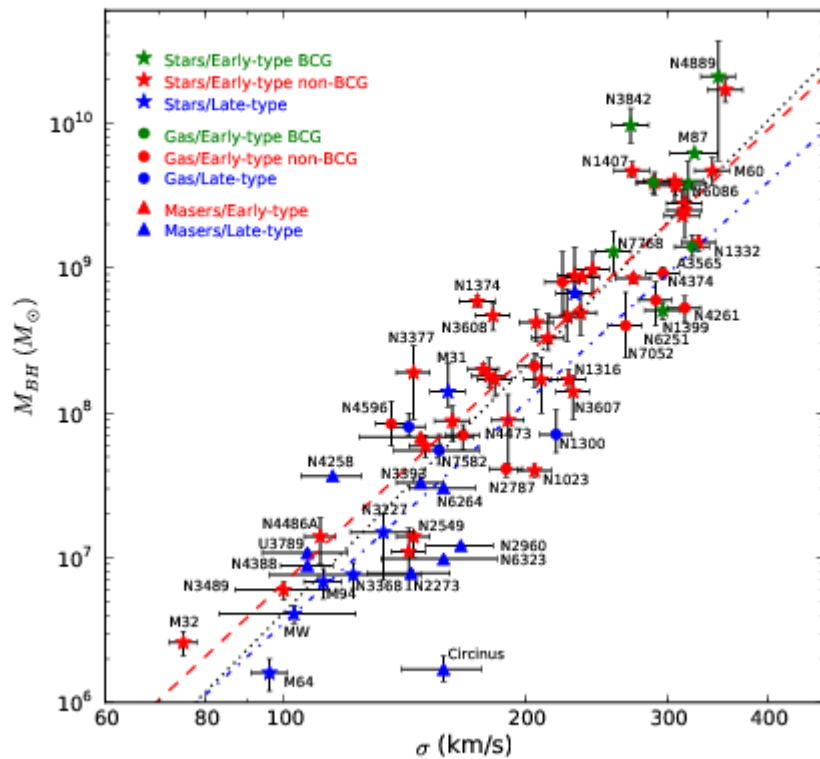
*TDE event (Holoien et al. 2014).*

## 9. Interaction between the nucleus and the rest of the galaxy

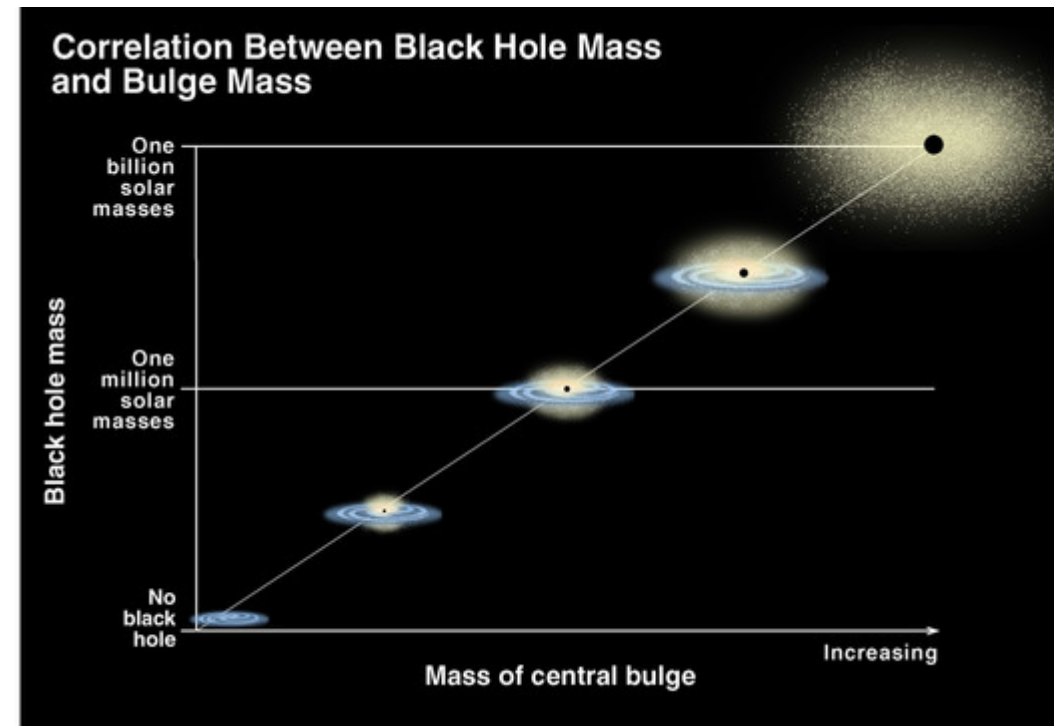
It is well established observationally. We see a close relation between the black hole mass and the bulge mass of the host galaxy, first discovered as Magorrian relation

$$M_{BH} = 0.0012 M_{bulge}$$

It implies the co-evolution of the black hole and the host. The exact physics of the feedback is still under discussion.



Newer diagram with data from McConnell & Ma (2013), using the dispersion velocity as a proxy for the bulge mass.

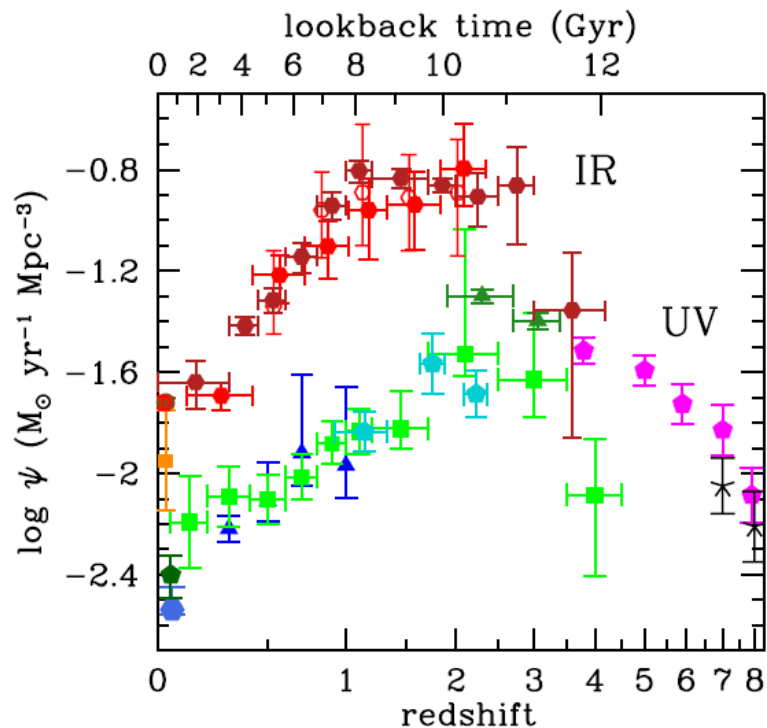


Artistic illustration; Credit: K. Cordes & S. Brown (STScI)

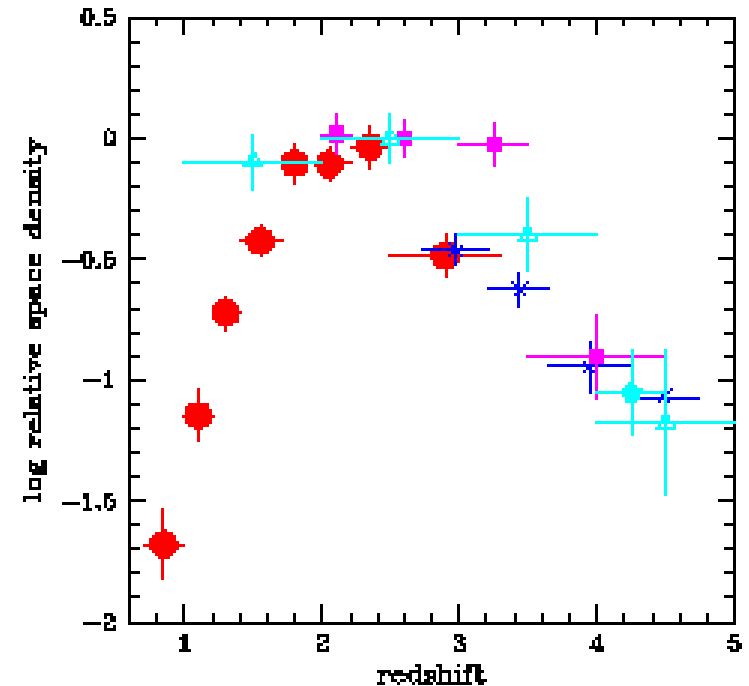


## 9. Interaction between the nucleus and the rest of the galaxy

Both the quasar number density and the star formation rate (SFR) peak at about redshift 2. There is no clear shift, but star formation must happen BEFORE the quasar activity since the metallicity of quasars is always solar or super-solar, even at the highest redshifts.



Star forming rate in the comoving frame  
(Madau & Dickinson 2014)



The evolution of the quasar density in the comoving frame (Madau, <https://ned.ipac.caltech.edu/level5/Madau/Madau7.html>)

**AGN activity is needed to model properly the formation of galaxies consistently with the observational data – without AGN feedback galaxies evolve too quickly. AGN provides the energy input which moderates star forming rate.**

# Summary

- In AGN we have the additional problem of the complex interaction with a host
- We do not handle well the evolution although large statistics of AGN helps
- We meet the same problems as before with jet formation and the transition between Keplerian disk/inner hot flow but overall similarities are obvious

**No homework**